Tasmania

Tasmanian Geological Survey
Record 1993/28

Geological setting and petrochemistry of Eocambrian–Cambrian volcano-sedimentary rock sequences from southeast King Island

by H. M. Waldron[1] and A. V. Brown

Abstract

Three distinct basaltic lava-sedimentary rock associations are exposed along the southeast coast of King Island. These volcanic suites are considered to represent three partial melting events of a heterogeneous mantle source or sources.

The first of the volcano-sedimentary rock sequences formed during a rifting phase within continental lithosphere. Initiation of rifting was marked by a change in sedimentation and the extrusion of pyroxene-phyric, tholeiitic, pillowed and massive lava flows with associated volcaniclastic units. The lavas are characterised by low Ti and Zr contents with variable LREE enrichment, suggesting that they were derived by partial melting of a depleted mantle source, enriched with a LREE fraction.

The second association consists of picritic pillow and tabular flows with associated breccia and hyaloclastite units and thin sedimentary beds. This picritic suite disconformably overlies the lower tholeiitic sequence. The chemistry of the lavas indicates that they were derived from a depleted, refractory mantle source.

The third sequence is a volcano-sedimentary rock association with tholeiitic lavas and consists of interbedded lava units and volcaniclastic mass flows. Chemically, the lavas within this succession are not depleted in incompatible trace elements and were probably derived from low degrees of mantle melting with residual clinopyroxene and garnet. Dykes of this third sequence intrude rocks belonging to both the earlier tholeiitic and picritic volcanic phases.

Past assumptions of a direct correlation with volcano-sedimentary successions in the Smithton Basin of northwestern Tasmania are not substantiated, but some similarities do exist within part of the lower sedimentary rock association.

1. Department of Geology, University of Melbourne, Parkville, Victoria 3052
Present address: Becquerel Laboratories Pty Ltd, PMBI, Menai, NSW 2234

INTRODUCTION

This paper presents the results of the first comprehensive study of the stratigraphy and geochemistry of the volcano-sedimentary rock successions which make up the southeastern corner of King Island. These rocks have been assumed by past writers to be of Eocambrian–Cambrian age.

An understanding of the physical relationship and chemistry of the volcanism on southeastern King Island provides important constraints for tectonic models of this area. This is important in view of the recently proposed tectonic models for Tasmania (Crawford and Berry, 1992), and its relationship with Northern Victoria Land, Antarctica, to the south (Findlay *et al*., 1991) and Victoria to the north (Crawford *et al*., 1984). Previous studies of the area have implied a direct relationship between the volcano-sedimentary successions on King Island and those in the Smithton Basin. Data presented here suggest otherwise.

The well-exposed volcano-sedimentary associations along the southeast coast of King Island (fig. 1) provide an excellent opportunity to observe the products of three different types of volcanism probably formed during intracontinental rifting. Sedimentary rock successions of sandstone, siltstone, mixtite and dolomite are overlain by three distinct volcano-sedimentary associations. The earliest volcanic phase consists of tholeiitic lavas intercalated with sedimentary rocks. This phase is disconformably followed by a picritic lava phase, and then by a second tholeiitic sequence.

The volcanic rocks in this area of King Island have previously been investigated by Scott (1951) and Solomon (1969), who concentrated on the petrography of the rocks and the mechanism of formation of the pillow lavas respectively. Scott (1951) recognised a tholeiitic and picritic association, but field divisions of these two groups of volcanic rocks were poorly defined. Neither of these workers recognised the upper tholeiite sequence.

In this paper we present the regional geology, petrology and chemistry of the three volcanic associations, and suggest possible source environments for the magmas.

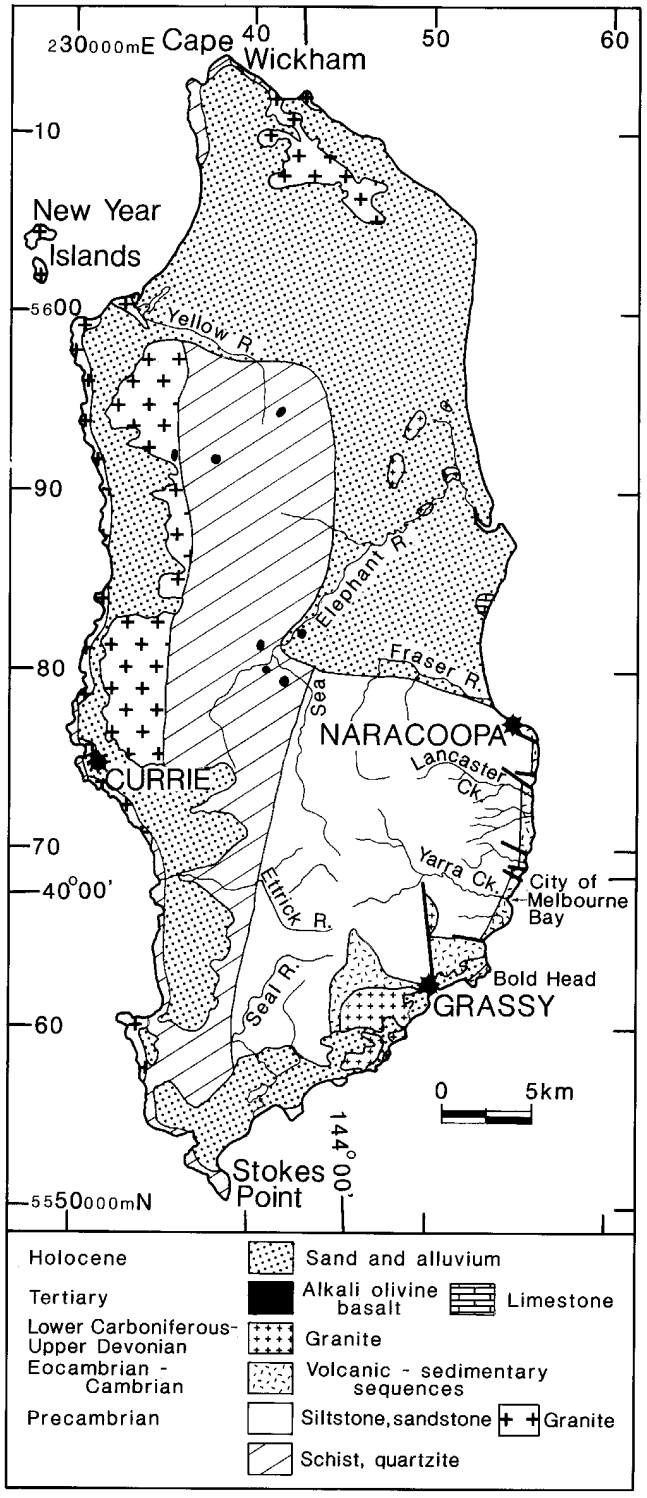

Figure 1
Geology of King Island (modified from Jennings and Cox, 1978)

REGIONAL GEOLOGY

The oldest rocks on King Island crop out on the west coast and form part of a multiply-deformed Precambrian basement complex consisting of metasedimentary rocks and regionally concordant granitic bodies (fig. 1). The metasedimentary sequence is more than 6000 m thick (Danielson, 1975) and consists predominantly of quartz-muscovite schist and quartzite, striking uniformly north and dipping west. The granitic rocks consist of biotite granite and granodiorite, dated at 750 Ma (McDougall and Leggo, 1965). These rocks have been extensively sheared, in places display gneissic texture (Gleadow and Lovering, 1978), and have associated aplitic, pegmatitic and minor amphibolitic dykes.

An inferred unconformity separates the metamorphic complex from a sequence of relatively unmetamorphosed argillaceous sedimentary rocks, presumed to be of Precambrian age, which form the majority of the eastern half of King Island. The regional strike of this sequence is north–south, with an easterly dip (Danielson, 1975). Along the southeast coast the

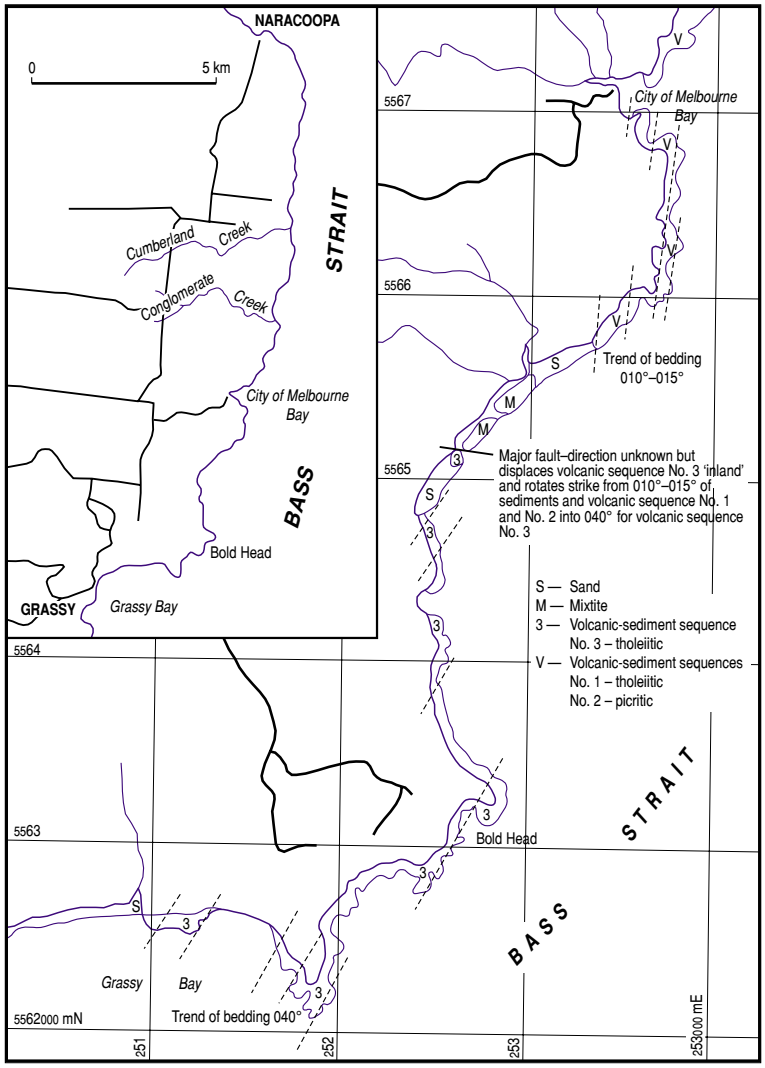

Figure 2

Location map (inset) and bedding trends in the southeast coastal sequence

A variety of dykes transect the southeastern coastal sequences (fig. 3). These include dykes with picritic and tholeiitic compositions associated with volcanism, as well as thick syenitic intrusions of unknown age, and later lamprophyric dykes which have been dated at 143 Ma (Gleadow and Duddy, 1980). Three small granite stocks and associated aplitic and pegmatitic dykes (dated at c. 350 Ma, McDougall and Leggo, 1965; Gleadow and Lovering, 1978; Brown, 1990) also crop out along the east coast (fig. 1). Two of these stocks intrude the southern extension of the volcano-sedimentary sequences, where the contact metamorphic equivalents form the Grassy Group (Knight and Nye, 1953). Scheelite skarn mineralisation, formed by selective metasomatic replacement of carbonate horizons (Large, 1971; Danielson, 1975; Kwak, 1978), occurs in the contact metamorphic aureoles of the Grassy and Bold Head intrusions.

Tertiary limestone beds near Naracoopa (fig. 1), described by Chapman (1912) and Crespin (1945), and minor small occurrences of Tertiary alkali olivine basalt, are the youngest rocks known on the island.

relatively unmetamorphosed sequence is overlain, with apparent conformity, by a sequence of sandstone, siltstone, mixtite, dolomite, tuff and mafic volcanic rocks (fig. 1, 2), assumed to be of Eocambrian–Cambrian age because of lithological similarities with rock successions in the Smithton area of northwestern Tasmania.

This latter sequence is well exposed along a 10 km section between Cumberland Creek and Bold Head (fig. 2, 3). Its regional strike is approximately 010° in the north and central parts of this area, and 040° towards Bold Head in the south. Dips of approximately 50°E are fairly constant throughout the area. The sequence exhibits considerable lateral variation in both thickness and lithology.

The sedimentary successions are followed by at least three distinct mafic volcano-sedimentary associations. The earliest volcanic phase consists of pyroxene-phyric tholeiitic lavas. These are followed discordantly by a sequence of picritic flows with intercalated breccia and hyaloclastite units. The picritic sequence is followed by a second tholeiitic lava phase, with interbedded volcaniclastic conglomerate units, which crop out in the Bold Head region. This second tholeiitic sequence is not observed in physical contact with either of the earlier volcanic rocks, but dykes associated with the later phase cut both the picritic and earlier tholeiitic successions.

GEOLOGICAL RELATIONSHIPS WITHIN THE EOCAMBRIAN–CAMBRIAN SEQUENCE

Sedimentary Successions

Siliceous sandstone–laminated siltstone

The lowermost of the presumed Eocambrian sedimentary rock successions exposed in the Cumberland Creek–Bold Head area consists of predominantly clean, well-bedded, shallow water, medium to coarse-grained sandstone (with bed thicknesses ranging up to 700 mm), interbedded with fine-grained muscovitic quartz sandstone which, in places, contains crossbedding. In the upper part of this succession progressively thinner sandstone units are interbedded with siltstone. The boundary between the dominantly sandstone and dominantly siltstone horizons (exposed in Cumberland Creek) is marked by a one metre thick pebble conglomerate band composed mainly of rounded quartzite clasts. The overlying laminated siltstone is uniform, both laterally and vertically.

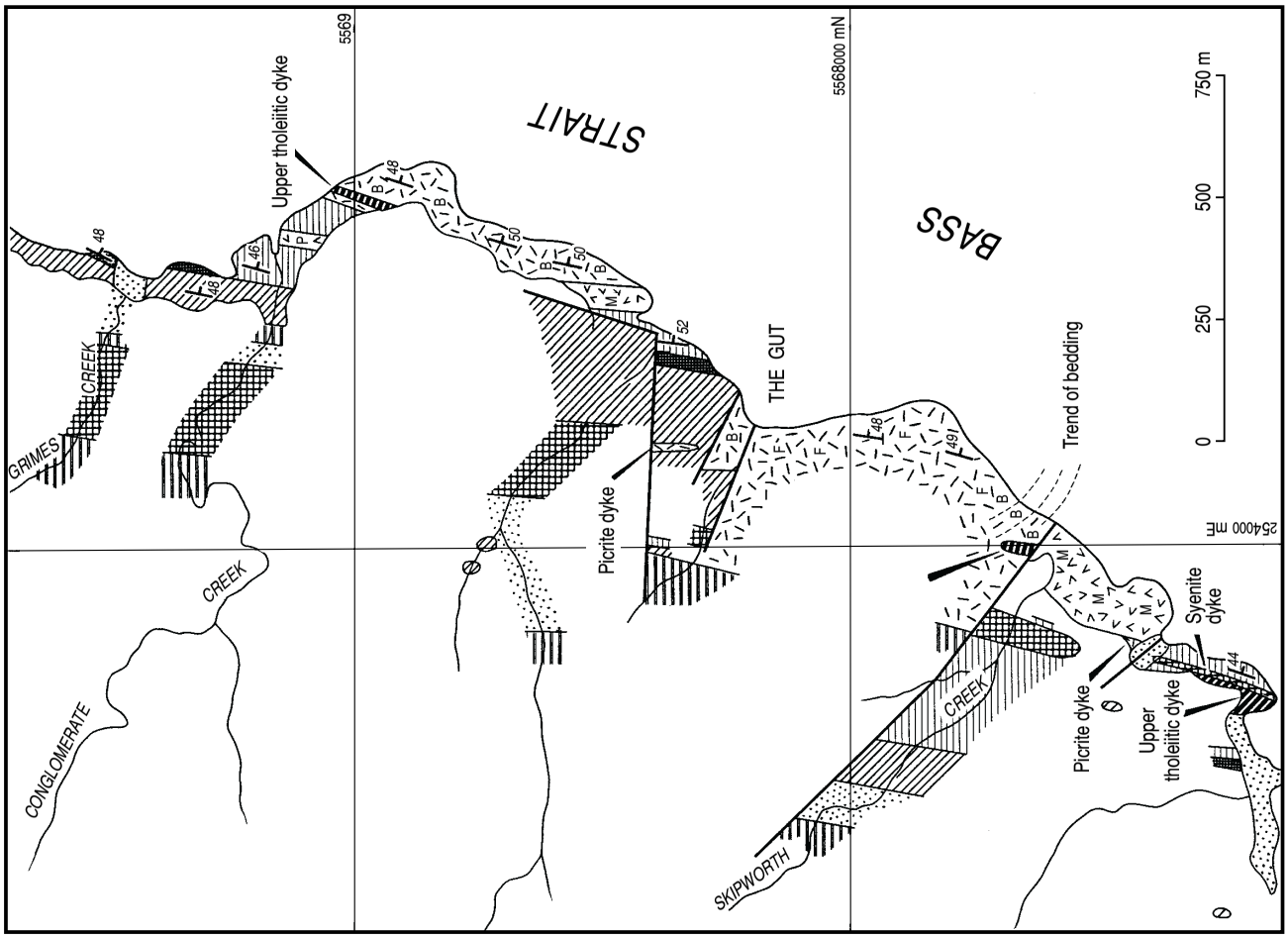
STRAIT
BASS
5569
5568000 mN
Upper tholeiitic dyke
THE GUT
Picrite dyke
Trend of bedding
Syenite dyke
Picrite dyke
Upper tholeiitic dyke
GRIMES CREEK
CREEK
CONGLOMERATE
SKIPWORTH
CREEK
254000 mE
0
250
500
750 m

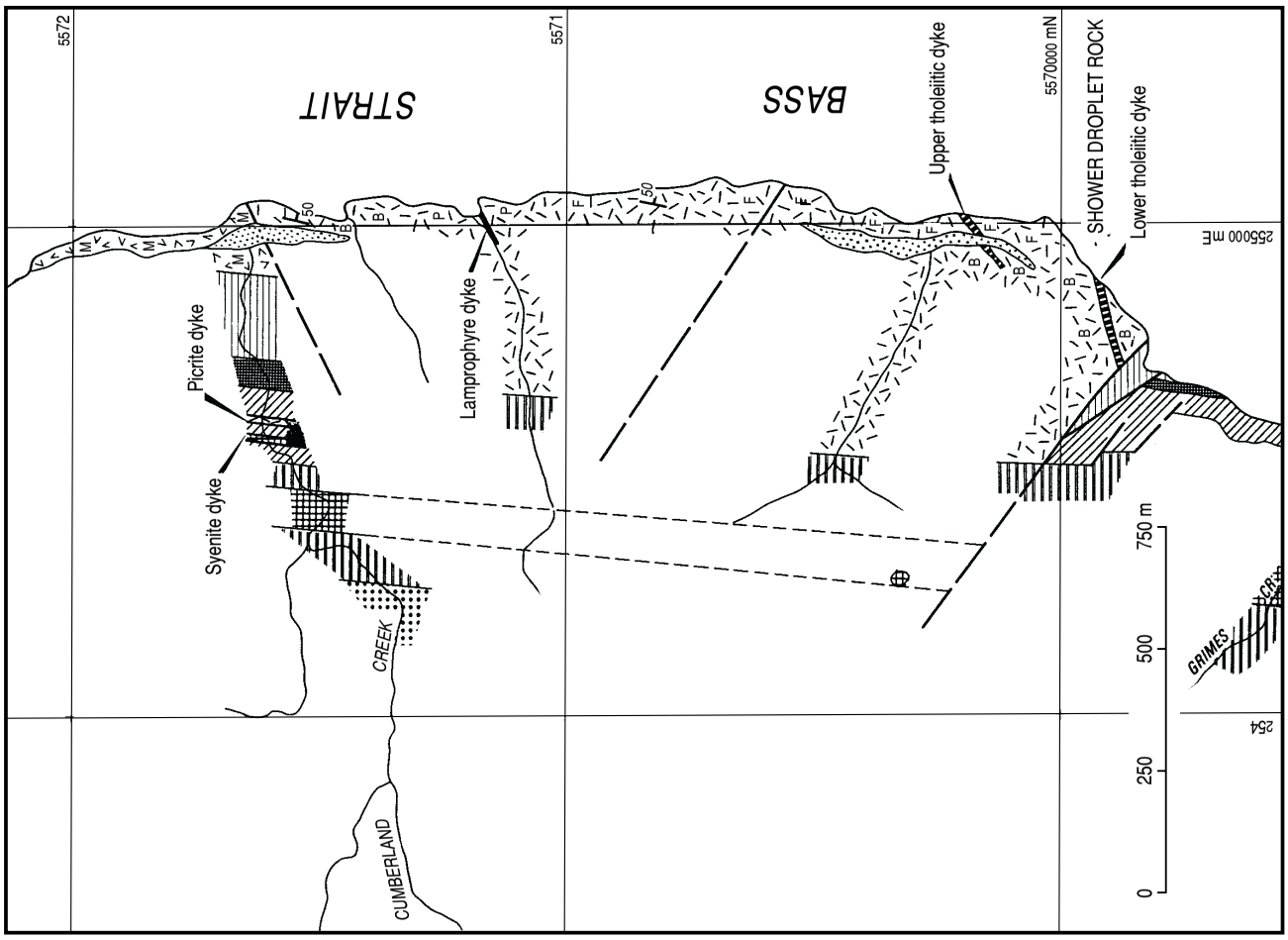
STRAIT
BASS
5572
5571
5570000 mN
Upper tholeiitic dyke
SHOWER DROPLET ROCK
Lower tholeiitic dyke
Picrite dyke
Lamprophyre dyke
Syenite dyke
CREEK
CUMBERLAND
GRIMES
CREEK
255000 mE
254
0
250
500
750 m

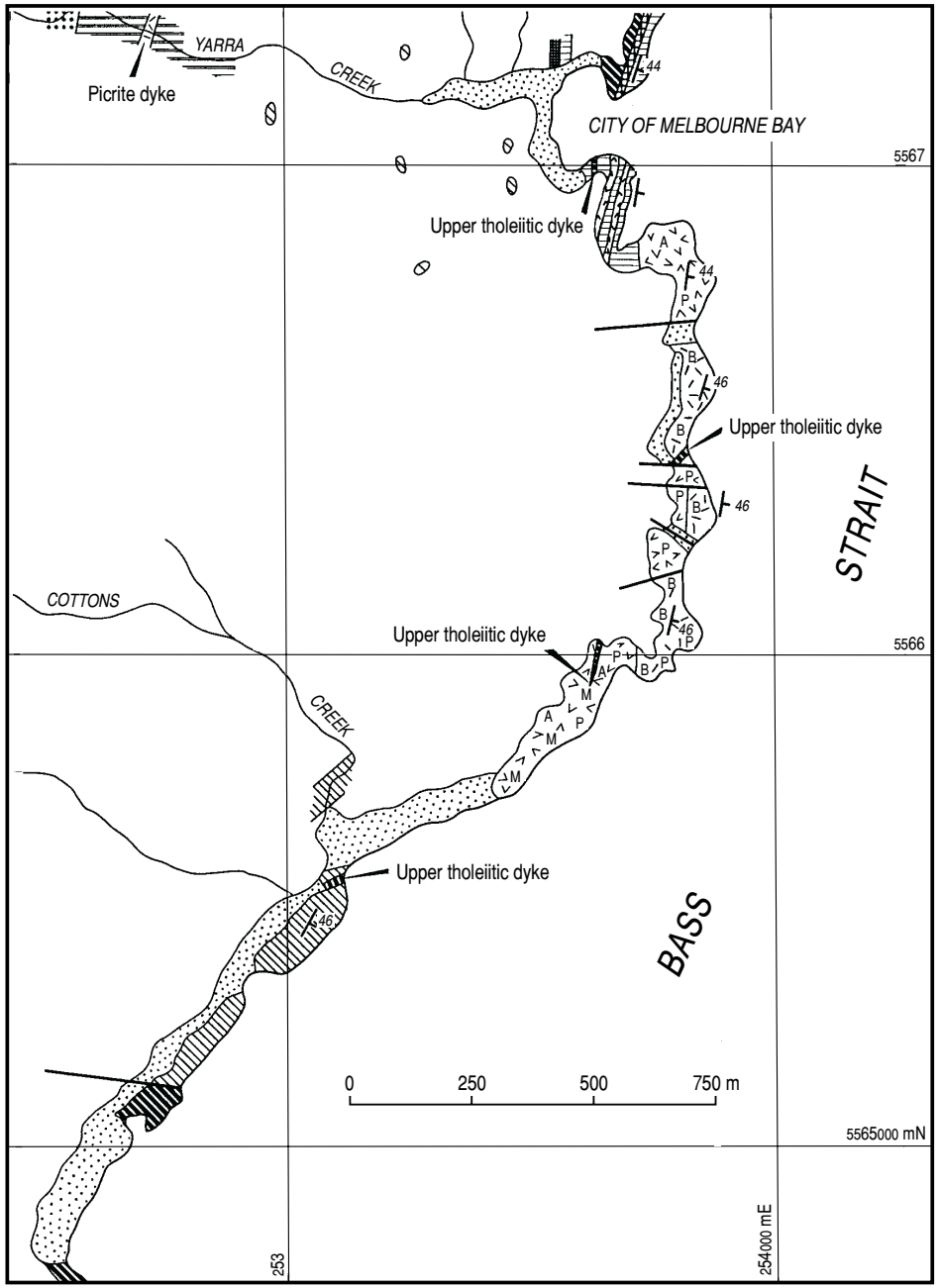

LEGEND

- Pebble and sand beaches and alluvial cover
- Upper tholeiites: Interbedded porphyritic and non-porphyritic flows, conglomerate and chert
- Picrites
  - P — Predominantly pillow lavas
  - F — Predominantly thick flows
  - B — Predominantly thin flows, breccias and hyaloclastites
- Lower tholeiites
  - P — Pillow basalts
  - M — Massive basalts
  - A — Agglomerate and tuff
- Siltstone and tuff with tholeiite flows
- Dolomite
- Mixtite
- Laminated siltstone
- Siliceous sandstone

Dykes

- Lamprophyre dyke
- Syenite dyke
- Tholeiite dyke
- Picrite dyke
- Fault
- Inferred fault
- Dip and strike (44)

Figure 3

Geological map of southeast King Island

Mixtite

The siltstone sequence grades upwards into what has previously been referred to as a tillite (Waterhouse, 1916; Carey, 1947), tilloid (Large, 1971) and breccia (Jago, 1974). The unit is best described as mixtite, a term proposed by Schermerhorn (1966) to describe a sedimentary rock "...with mixed, ill-sorted, dispersed megaclastic lithology with a great to extreme range in size grades, without regard to its composition or origin".

The mixtite consists of poorly-sorted, crudely stratified flows which vary considerably in lithology (fig. 4). Clasts within the mixtite are dominantly subangular, but vary from subangular to subrounded, and were derived from a quartzite, meta-siltstone and carbonate-bearing terrain. They are set in either a red hematitic or a grey calcareous matrix. The coarser clasts (200–300 mm) are generally quartzite and metasiltstone. Carbonate clasts tend to be smaller (approximately 50 mm), although one large rip-up clast, approximately 3 m across, is considered to have been locally derived from interbedded carbonate units in The Gut area (fig. 3). Minor clasts of red jasper, banded chert and rip-up mudstone fragments are also found at The Gut, with quartzite conglomerate clasts being more common in the Conglomerate Creek–Grimes Creek area (fig. 3). The mixtite is largely matrix supported, but contains minor, interbedded, clast-supported flows.

Several truncated lenses of graded sandstone-siltstone are interbedded with the mixtite (The Gut and Cottons Creek areas, fig. 3). Some of these lenses consist of 10–100 mm thick beds of coarse-grained sandstone containing rip-up clasts, grading up into siltstone which exhibits truncated cross bedding in places (Cottons Creek). Vitric-lithic tuff horizons, containing dominantly glass shards and dacitic lava clasts set in a calcareous matrix, are interbedded with the mixtite (The Gut and City of Melbourne Bay, fig. 3). The tuffaceous horizons also display well developed cross bedding at some localities (Cottons Creek).

In places, the upper part of the mixtite succession consists of pebble-grade quartzite clasts in a red sandstone matrix, and numerous lenses of graded sandstone with cross-bedded tops (Cotton Creek). A boulder horizon occurs near the top of the mixtite at other locations (The Gut and Conglomerate Creek–Grimes Creek). At The Gut the boulder horizon is overlain by a 500 mm thick unit of hematitic sandstone.

The mixtite is considered to have been formed by density flow and is not, as previously considered, of glaciogenic origin (Waterhouse, 1916; Carey, 1947). Features such as grading and cross bedding, infilled scours, and interbedded tuffaceous horizons are inconsistent with a glaciogenic origin or sediment redeposited from ice-rafted debris. The non-glaciogenic origin is also supported by the outcrop of the mixtite within the succession being restricted to the southeast of King Island. A single striated pebble found in the mixtite sequence by Carey was the basis of the proposed glacial origin. However, as only one striated pebble has so far been found, it is considered here to have been reworked into the mixtite successions.

Figure 4

Coarse mixtite showing grading. Clasts are mainly quartzite, chert and metasiltstone in a hematitic matrix. Locality: The Gut

Carey (1947) also interpreted associated laminated dolomite as varves, and correlated the unit with the Adelaidean series glacial sediments. The mixtite of southeast King Island is clearly unlike the Adelaidean series glacial sediments which occur in both the Kimberley region, where abundant striated, faceted and polished boulders are associated with underlying glacial pavements (Coats and Preiss, 1980), and in the Adelaide Geosyncline, where numerous striated clasts (Coats, 1964; Cooper, 1973) of varied igneous, metamorphic and sedimentary rocks occur (Campana, 1958; Thomson, 1969; Coats, 1971).

The mixtite has also been described by Jago (1974) and reviewed by Rankama (1973), both of whom doubted a glacial origin. The formation name `Cottons Breccia' (Jago, 1974) is inappropriate, as the sequence consists of mixtite, not breccia, and the Cottons Creek section is atypical of the unit as a whole. Future use of this formation name is not recommended.

Dolomite

The mixtite succession is conformably overlain by laminated and thinly-bedded dolomite in The Gut and Conglomerate Creek–Grimes Creek areas, and by silicified dolomite at City of Melbourne Bay. In Cumberland Creek the mixtite grades into calcareous mudstone, without a distinct dolomite horizon. The dolomite is finely laminated, with layers up to 1–3 mm in thickness, with some well-developed cross and truncated laminations associated with channel fill structures. Finely disseminated hematite causes the dolomite to vary in colour from grey to pink.

Remnant oolite and pellet textures and microstylolites are visible within the dolomite units, suggesting early diagenetic dolomitisation of limestone. These relict limestone textures, and the associated calcareous mudstone, suggest deposition in a subtidal to intertidal environment (Williams, 1979). No evaporite minerals, or their pseudomorphs, have been found, suggesting that dolomitisation took place in an intertidal area where evaporite minerals were not preserved, rather than a hypersaline supratidal environment (Illing *et al*., 1965).

Siltstone-tuff sequence

The upper part of the sedimentary sequence along the southeast coast of King Island consists dominantly of interbedded laminated siltstone with minor volcaniclastic lithicwacke and tuff. The laminated siltstone varies in colour from black to grey and red. The grey siltstone is generally pyritic, while the red siltstone is uniformly laminated with 20–30 mm thick hematite-rich bands parallel to the lamination.

The onset of tholeiitic volcanism resulted in deposition of interbedded tuff and volcaniclastic lithicwacke units towards the top of the laminated siltstone sequence. The continuation of volcanic activity dominated the formation of laminated siltstone, forming agglomerate, tuff and volcanic breccia units, interbedded with minor siltstone, at the base of the tholeiitic pillow and massive basalt flows.

Volcanic Successions

Lower Tholeiite Sequence

The early phases of tholeiitic volcanism intruded hydroplastic sediments, resulting in the incorporation of tongues of siltstone in the basalt flows (fig. 5*a*). Agglomerate lenses, at times associated with feeder necks, crop out at several locations along the coast. The largest of these is just south of the City of Melbourne Bay (fig. 3), where subangular amygdaloidal basalt blocks and chert fragments discordantly cut red siltstone and are overlain by 30 m of finer grained, graded agglomerate.

Tuff horizons overlie the basal agglomerate. These tuffs are dominantly medium-grained lithic-vitric or lithic-crystal varieties containing fragments of tholeiitic basalt and dacitic lavas, plagioclase and pyroxene crystal fragments, devitrified glass and quartz grains. The tuff horizons exhibit characteristic features of redeposition by turbidity currents.

The lava phase of the lower tholeiite sequence is dominated by massive and pillowed basalt flows with only minor, interbedded, siltstone and tuff units. Both massive and pillowed basalt occur as discrete flows, and pillow structures sometimes occur either at the top or base of the massive flows.

Pillow shapes vary considerably. The smaller pillows occur individually (fig. 5*b*) or as interconnected sac and neck types (fig. 5*c*), with subspherical to ellipsoidal cross sections and ranging in diameter from 50 mm to one metre. The larger pillow structures, up to four metres long, are mattress-shaped (fig. 5*d*) and similar to the mega-pillows described by Dimroth *et al*. (1978) and Jackson (1980).

The smaller pillows are generally zoned, with a dark green devitrified glass rim passing into an amygdaloidal zone, with radially arranged amygdules, and a variolitic core. Individual pillows are set in a devitrified glassy matrix and are now largely composed of chlorite, serpentine and epidote. Some of the pillows have quartz-filled interiors which may represent infilling of small lava tubes. The units of smaller pillows are extensively veined with epidote and minor quartz, and are associated with only minor brecciated pillow fragments and hyaloclastites. In contrast, the large mattress-shaped pillows have only a thin, chilled outer margin and no glass rim or amygdaloidal zone. They are usually stacked in contact with each other, without inter-pillow material, but occasional small pillow-infill triple junctions do occur between the mega-pillows. Veining is minor and no hyaloclastites are present.

The formation of individual or interconnected pillow types is probably dependent on the rate of movement of the flows. The budding and necking, where spherical sacs have not separated, results from relatively slow movement of flows (Solomon, 1969; Dimroth *et al*., 1978). The mega-pillows probably formed from rapid voluminous extension of lava in deeper water, with each mattress-shaped pillow representing successively emplaced lava tubes.

Picrite Sequence

A thick sequence of picritic rocks disconformably overlies the lower tholeiite succession. Pillow lavas, flow units, breccia and hyaloclastite units have been distinguished. The picritic pillows, unlike those of tholeiitic composition, are not zoned and occur as irregular subspherical units, about 250 mm across, or as elongate cylindrical tubes with smaller interconnected pillow buds and branches (fig. 6*a*). Some pillow lavas have wrinkled surfaces similar to subaerial pahoehoe lavas. Flattened, layered pillow structures occur and are generally about 400 mm across, having a 150 mm outer shell and subhorizontal internal layering. These flattened shapes are considered to be infilled lava tubes.

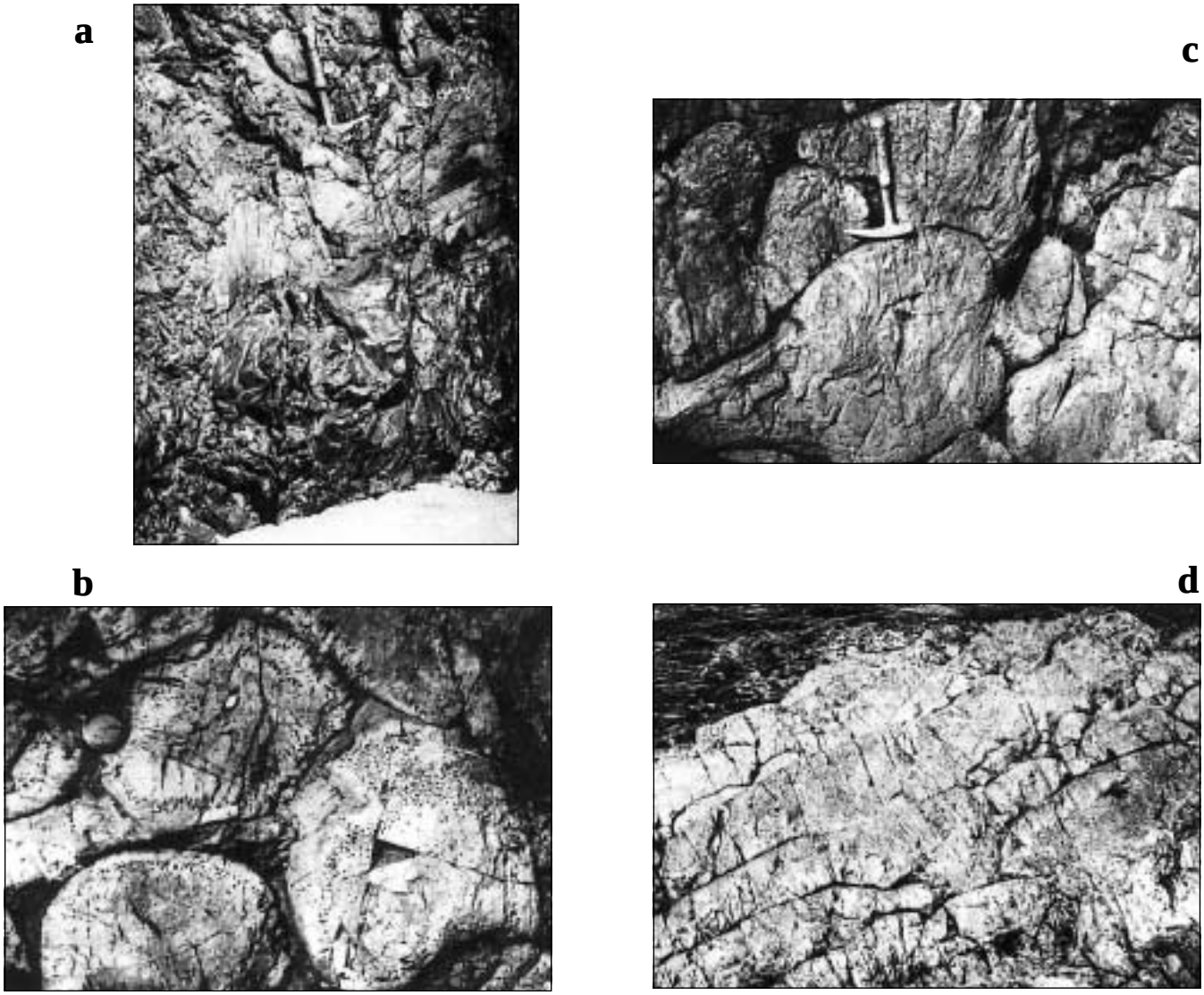

Figure 5

(a) Massive basalt of the lower tholeiitic sequence intruding hydroplastic red siltstone;
(b) Pillow basalt of the lower tholeiitic sequence showing individual pillows prominent rim, amygdaloidal and core zones;
(c) Interconnected zoned pillows of the lower tholeiitic sequence;
(d) Megapillows of the lower tholeiitic sequence showing mattress-shaped pillows up to four metres long.

Pillow lavas are common towards the top part of the exposed picritic succession.

Picritic flow units occur either as thick, uniform flows or thin, brecciated flows. The thick flow units vary between 500 mm and two metres in thickness and crop out over a considerable area north of City of Melbourne Bay and Shower Droplet Rock (fig. 3). Individual flows often have chilled bases, and in some cases have both chilled bases and tops (fig. 6*b*). Minor amygdaloidal flows occur within the thick flow succession. In places the flow units grade along strike into dominantly pillow and breccia structures.

Unlike the uniformity of the pillow lava and thick flow units, the thin flows, breccia and hyaloclastite units are variable in thickness and occur as interbedded sequences (fig. 6*c*). Thin flows (20–50 mm thick) commonly occur as broken and contorted lenses and rafts in a hyaloclastite matrix. Some thicker flows (up to 500 mm thick), with sinuous outlines and hollow interiors (fig 6*d*), are considered to be preserved lava tunnels. Local intrusive relationships with associated hyaloclastite units are common (fig. 6*e*). Picrite breccia fragments in a hyaloclastite matrix vary in size from a few centimetres up to two metres across, but are generally between 100 and 200 mm across. As with the picritic pillows, these breccia fragments are not zoned.

Hyaloclastite units consist of devitrified picritic glass shards and lava granules. They occur either as matrix to the thin flows and breccia fragments, or as individual graded or finely-laminated units, some of which contain cross bedding. Soft-sediment deformation features, such as convolute bedding, slump structures and intraformational rip-up clasts, indicate that some of the hyaloclastite units were redeposited by turbidity currents.

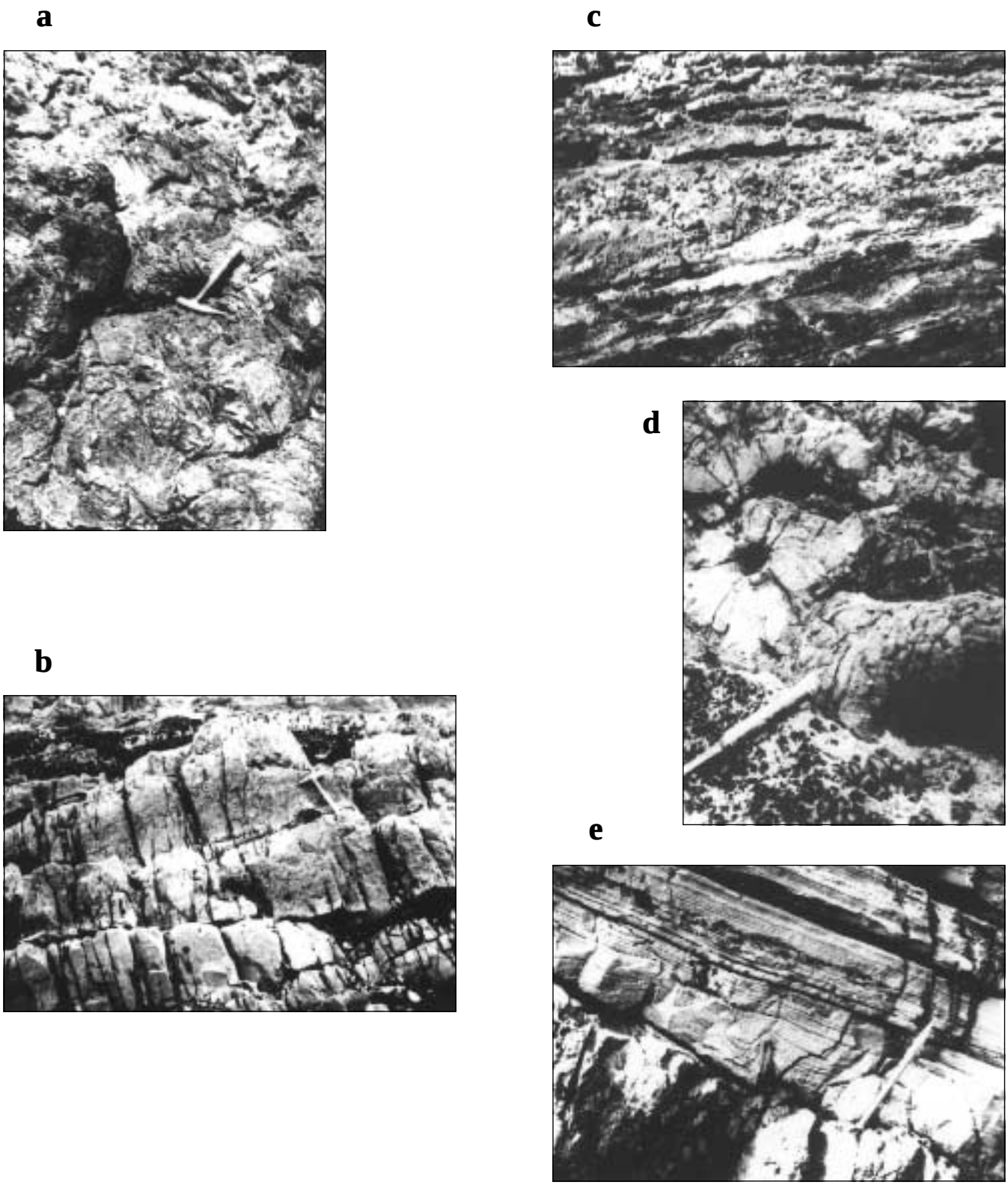

Figure 6

(a) Picritic basalt;
(b) Thick picritic flows with chilled bases and tops;
(c) Picritic breccias, thin flows and hyaloclastites;
(d) Picritic lava tubes;
(e) Laminated picritic hyaloclastite.

The variation in morphology of the various picritic units is best explained by the eruption of different volumes of picritic lava, at variable rates, from proximal vents onto an irregular seafloor. The volume and rate of supply of lava largely determines the intensity of quenching. Rapid extrusions of large volumes of lava are likely to have formed the thick flow units, whereas slower extrusions of similar proportions allowed time for budding and branching pillows to form. In both cases the lava/water ratio is large, resulting in minimal interaction. In contrast, the thin flows and breccia and hyaloclastite units probably formed by the increasingly intense interaction of seawater with progressively smaller volumes of lava, resulting in a greater degree of granulation. Partially intrusive flow lenses display little fragmentation, probably as a result of their protective hyaloclastite cover.

Granulation has been widely suggested as a mechanism for hyaloclastite development (Parsons, 1969; Solomon, 1969; Grobler and Botha, 1976; Honnorez and Kirst, 1976; Dimroth *et al*., 1978; Schmincke *et al*., 1979). The chemical composition of the picritic units on King Island is uniform, consistent with the morphological variations having resulted from a syn-eruptive process such as granulation. Autobrecciation probably also contributed to fragmentation, and spalling from pillow and flow margins, as described by Rittman (1962) and Moore (1975), may have occurred. However, the volume of hyaloclastites is too large for them to have formed mainly by this mechanism. The King Island picritic units are morphologically similar to modern and ancient examples thought to have formed by granulation, such as the Mid-Atlantic Ridge rift valley near the Azores Plateau (Ballard and Moore, 1977), hole 346B of the DSDP Leg 36 (Schmincke *et al*., 1979), and Archaean volcanic rocks in the Rouyn–Noranda area of Quebec (Dimroth *et al*., 1978). These basalts are all of tholeiitic composition, which suggests that the granulation process for the formation of the King Island picrite sequence is a function of seawater interaction with lava, independent of composition.

The thick picritic flow units are often vesicular, suggesting that they formed in relatively shallow water. Although the pillow flows, breccia units and thin flows are poorly vesicular, their minor association (gradational boundary at one locality) with vesicular flows raises the possibility that the fragmentation may have resulted from explosive mechanisms. Vesiculation due to explosive escape of exsolved magmatic gas is unlikely, in view of the picritic composition, but a phreatomagmatic process, caused by the vaporisation of seawater, is possible.

The similarity of the King Island hyaloclastite units with those described by Lonsdale and Batiza (1980) from a modern seamount near the East Pacific Rise, forming at depths too great for explosive activity, reinforces the idea that granulation was the main mechanism in the formation of the King Island breccia and hyaloclastite units. The poorly vesicular nature of the pillows and breccias suggests that they formed in a deeper part of the basin than the thick flows.

A subaerial 'lapilli tuff' described by Scott (1951) from Shower Droplet Rock (an area of interbedded thin flows, with breccia and hyaloclastite units; fig. 3) was not found. Abundant variolites, as found throughout the picrite sequence, developed as well-defined 'ball' textures up to 20 mm across. The weathering structures of these variolites may have been misinterpreted as lapilli.

Upper Tholeiite Sequence

A second tholeiitic sequence forms the youngest volcanic succession in the area and is exposed along the coast from south of Cottons Creek to Bold Head (fig. 2, 3). This upper tholeiitic sequence consists of porphyritic and non-porphyritic flows. The non-porphyritic flows have uniform bases and amygdaloidal tops, and both types of flow are associated with volcaniclastic conglomerate and hematitic chert.

The flows occur in repetitive cycles interbedded with 4–5 m thick beds of pebble-cobble grade conglomerate. This conglomerate consists of ellipsoidal to rounded volcanic clasts derived from the underlying flows, grading into finer granule conglomerate, hematitic mudstone and chert. The upper tholeiite sequence has not been previously recognised, and its relationship to the underlying tholeiite and picritic successions is based on dykes, petrochemically similar to the upper tholeiitic volcanic rocks, intruding the lower tholeiite and picrite sequences.

Dykes

Numerous dykes of both picritic and tholeiitic composition, as well as later syenitic and lamprophyric dykes, intrude the southeast coast volcano-sedimentary rock sequences. Picritic dyke varieties include quench-textured types, similar to the main picritic volcanic rocks, as well as cumulate and other varieties. Tholeiitic dykes, related to the upper tholeiite sequence, intrude the picritic, lower tholeiitic, and underlying sedimentary successions.

Several augite syenite dykes, which have an approximate north-south strike, are offset by faults in places (fig. 3) and cut the lower sedimentary rock succession. These dykes have previously been mapped as a single gabbro (Solomon, 1969) or dolerite (Jago, 1974) dyke at the base of the mixtite. Numerous thinner syenitic dykes, with variable trends, also occur in the area.

South of Cumberland Creek, a thin lamprophyre dyke (fig. 3) with chilled margins cuts across the picritic succession with a strike of 055°. Potassium-argon dates on similar intrusions were reported by McDougall and Leggo (1965). Recalculation of their data (using revised constants) by Gleadow and Duddy (1980) gave an age of 143 ± 3 Ma, which is 220–230 million years younger than the recently dated Late Devonian (~366–377 Ma) lamprophyre dyke suite in western Tasmania (Baillie and Sutherland, 1992; McClenaghan *et al*., 1994).

PETROGRAPHY AND MINERAL CHEMISTRY OF THE VOLCANIC SUITES

Lower Tholeiite Sequence.

The massive and pillowed basalts, forming the bulk of the lower tholeiite sequence, are very similar in composition and mineralogy. They consist of albitised plagioclase and fresh clinopyroxene with interstitial chlorite, titano-magnetite and epidote. Chemical analyses show the uniformity of the augitic clinopyroxene in both the massive and pillowed basalts (fig. 7). Most of the plagioclase present is albite which has been partially altered to sericite. Some fresh labradorite is preserved, particularly in the basal massive flows which are interbedded with siltstone. Green pleochroic chlorite (ripidolite variety) and epidote are abundant, and occupy interstitial positions and infill vesicles. Minor clinozoisite, quartz and patches of calcite are also present.

Textural criteria divide the massive basalt flows into ophitic and intergranular varieties. The ophitic varieties are occasionally coarse-grained (fig. 8*b*), with augite plates up to 5 mm across, although medium-grained varieties (augite grains 1-3 mm in length) are more common (fig. 8*a*). Medium-grained and fine-grained intergranular varieties consist of interlocking plagioclase laths (0.5–2 mm in length) with interstitial augite granules, together with abundant skeletal magnetite and chlorite. Finer grained varieties tend to be vesicular, with the vesicles being infilled with epidote and chlorite. Chalcopyrite, pyrite and pyrrhotite are common accessory minerals in the medium-grained rocks. The order of crystallisation of minerals forming the massive basalt flows is plagioclase with clinopyroxene, or plagioclase followed by clinopyroxene.

Zoned pillow basalt flows have devitrified glassy rims passing into progressively more crystalline interiors. Small diffuse patches of incipient crystallisation and small crystallites (about 0.1 mm in diameter) occur just inside the rim zone. Varioles (approximately 0.5 mm across) with hourglass and belt buckle-shaped plagioclase microlites, forming the nuclei for radially arranged quenched aggregates of pyroxene, are associated with minor small glomerocrysts of plagioclase in the amygdaloidal zone (fig. 8*d*). Towards the pillow centre, glomerocrysts of plagioclase laths (0.5–1 mm long) and smaller augite plates occur in a groundmass of radiating sheaves of clinopyroxene, plagioclase microphenocrysts (about 0.1 mm long), and interstitial magnetite (fig. 8*c*).

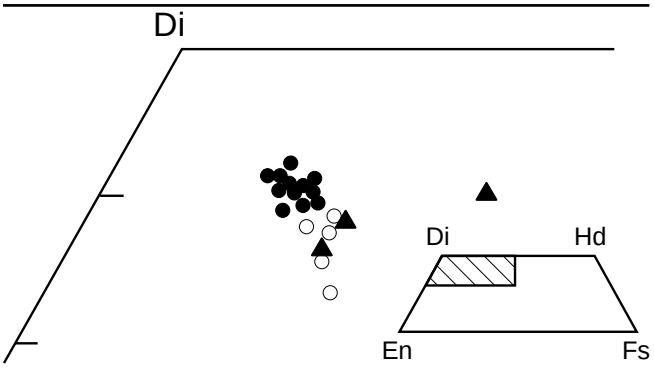

Figure 7

Pyroxene quadrilateral showing the composition of clinopyroxenes from the lower tholeiitic massive basalts (closed symbols) and pillow basalts (open circles). Massive basalt samples are: closed circles, ophitic; closed triangles, intergranular.

The elongate megapillows and the interiors of larger subspherical pillows consist of interlocking plagioclase laths (0.2–0.5 mm in length) with clinopyroxene groundmass and interstitial magnetite and chlorite. Some glomerocrysts of idiomorphic plagioclase (up to 1.5 mm in length) and subhedral augite grains (about 0.5 mm across) also occur. The order of crystallisation is the same as in the massive basalt flows, with plagioclase followed by clinopyroxene. Plagioclase in pillow basalt units has been completely albitised, probably due to extensive hydrothermal alteration by circulating seawater.

Picrite Sequence

The picritic lavas are usually porphyritic and consist of pseudomorphed phenocrysts after olivine (0.1–3 mm across) and small (0.05–0.2 mm) chromite euhedra in a quenched clinopyroxene-rich groundmass. In the pillow, breccia and thin flow units, the phenocrysts commonly range from hopper skeletal grains to euhedral crystals (fig. 9*a*) with apical angles and prismatic outlines indicative of olivine. All phenocrysts are completely pseudomorphed by colourless chlorite (pycnochlorite?). Other secondary minerals include abundant epidote, minor clinozoisite and small fibrous crystals, possible tremolite, with minor interstitial pyrite and chalcopyrite.

The chilled bases and tops of the thick flow units consist of chloritised olivine phenocrysts (0.5–1 mm), with small included chromite euhedra, together with arrowhead and chain and lantern-shaped clinopyroxene microphenocrysts, in a groundmass of radial lath, feathery and plumose-textured clinopyroxene (fig. 9*c*). The degree of crystallinity increases towards the centre of the flows, with idiomorphic olivine phenocrysts (up to 3 mm across replaced by serpentine and chlorite) and possible plagioclase microphenocrysts in a groundmass of coarse plumose to granular clinopyroxene grains (about 1 mm across) (fig. 9*d*). Magnetite commonly forms overgrowths on olivine and occupies interstices. The secondary minerals are the same as in the thin flow units, with the addition of calcite amygdales.

Some of the thick flows appear to be zoned, with an altered hyaloclastic base, consisting of 5 mm patches of devitrified glass, secondary quartz and magnetite in a chlorite matrix. This grades into zones of small euhedral pseudomorphed olivine phenocrysts in a

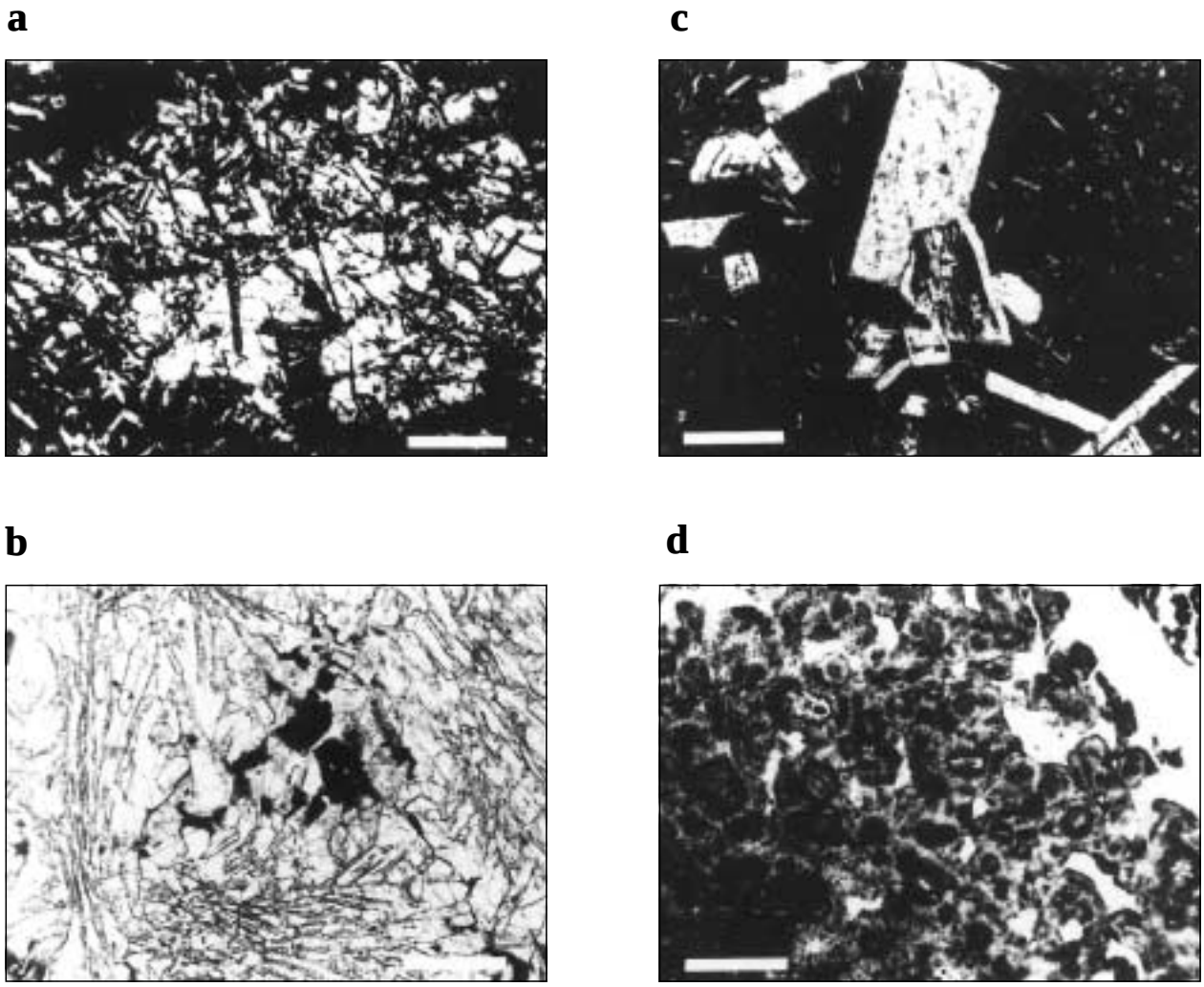

Figure 8

Photomicrographs of massive basalts and pillows of the lower tholeiitic sequence. Scale bar 500 μm.

(a) Ophitic texture in massive basalt.
(b) Coarse grained ophitic texture in massive basalt.
(c) Plagioclase and augite glomerocrysts in a quenched clinopyroxene groundmass from the core zone of pillows.
(d) Varioles in the rim zone of pillows.

radially-arranged sheaf clinopyroxene groundmass. These flows have vesicular tops, consisting dominantly of sheaf pyroxene and minor olivine phenocrysts.

Spherulitic textures are commonly developed in all the picrites, with spherulites ranging in size from 2 to 20 mm in diameter. The spherulites consist of radially-arranged sheaves of bladed clinopyroxene crystals, sometimes rimmed with feathery and dendritic clinopyroxene overgrowths. Spherulites occur either individually, particularly in the thick flow units, or coalesced (fig. 9*b*) forming a variolitic textured groundmass. The spherulites clearly represent rapid crystallisation as described by Dimroth and Lichtblau (1979) and Donaldson (1976), and not devitrification of glass (Lofgren, 1971; 1974) or immiscible liquid behaviour as described by Gelinas *et al.* (1976).

Texturally, the King Island picritic pillow and thin flows, breccia units and some of the thick flows, are similar to the Troodos upper pillow lavas and the volcanic rocks of the Agrilia Formation from the Othris ophiolite described by Cameron *et al*. (1980). The clinopyroxene morphology is similar to that in the groundmass described from Archaean (Arndt *et al*., 1977; 1979; Nisbet *et al*., 1977) and Mesozoic komatiites (Echeverria, 1980; Dietrich *et al*., 1981).

The hyaloclastite units consist of various sized granules of picritic lava, non-welded vitric shards, and clinopyroxene grains in a devitrified glass and chlorite matrix. The lava fragments are fine grained and texturally similar to the breccia and thin flows. The devitrified glass shards are angular and some have convex or concave boundaries with dark brown siliceous rims. Secondary epidote is common, with

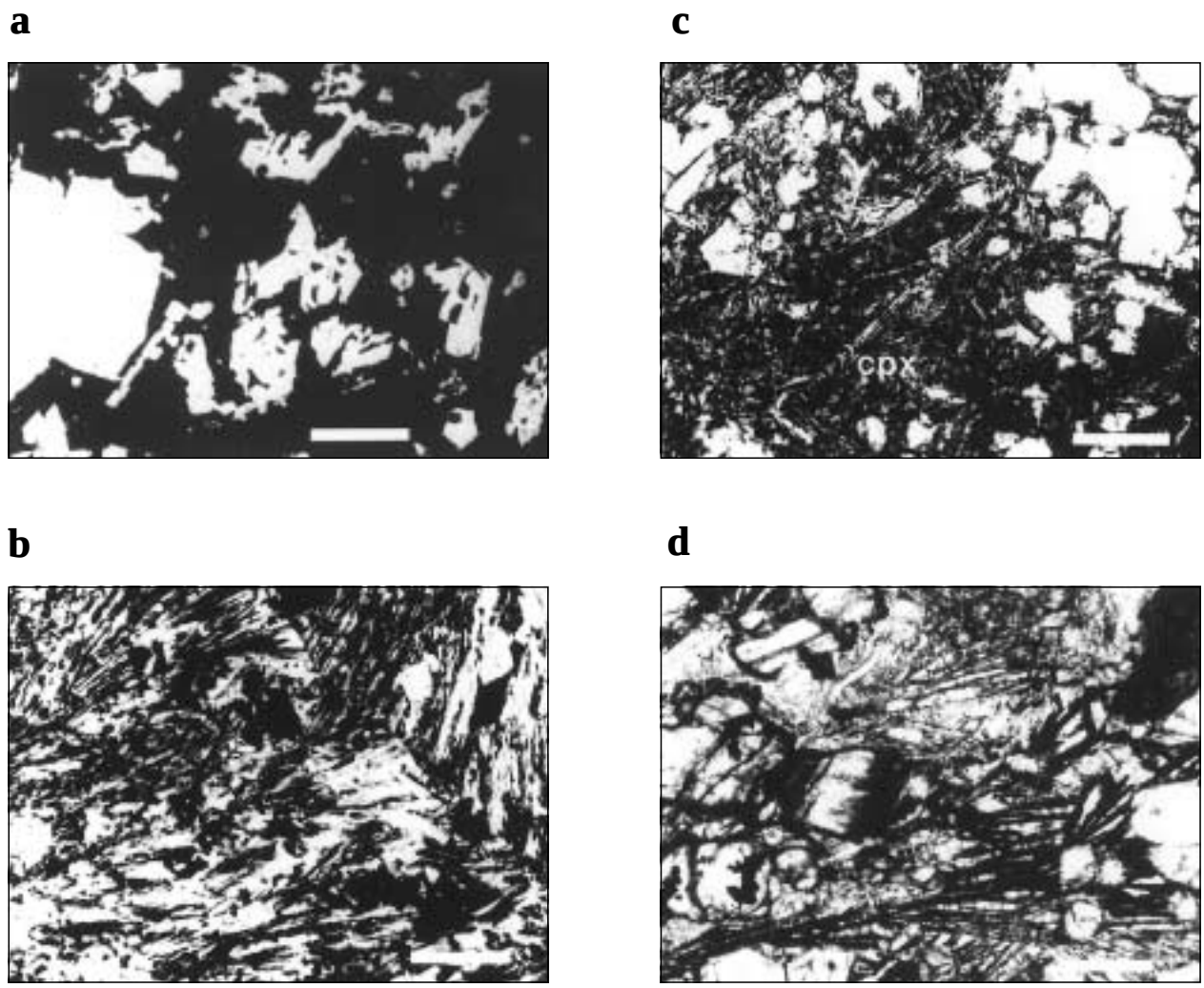

Figure 9

Photographs of the picrites. Scale bar 500 μm.

(a) Skeletal olivine phenocrysts completely pseudomorphed by colourless chlorite, common in the pillows, breccias and thin flows.
(b) Variolitic textures formed by coalescence of clinopyroxene spherulites.
(c) Olivine phenocrysts and clinopyroxene microphenocrysts in a quenched clinopyroxene groundmass, from the chilled base of a thick flow unit.
(d) Coarser grained plumose textured clinopyroxene from the central part of a thick flow.

accessory quartz and amphibole and irregular patches of calcite alteration.

Picritic dykes are generally texturally identical to the pillow flows and breccia units, but some cumulate types are present. The cumulate varieties are highly altered and consist of serpentinised olivine, with included chromite euhedra, and intercumulus pseudomorphs after pyroxene. A third textural variety of picritic dykes consists of graphic intergrowths of augite and albite, largely altered to sericite.

Clinopyroxene grains in the picrite flows are remarkably fresh. They are variable in composition and range from diopside and salite to augite (fig. 10). The greatest variations are displayed by Al_2O_3, CaO, SiO_2 and MgO (Table 1). Alumina contents increase with the degree of cooling rate of the crystals; coarse granular clinopyroxene has Al_2O_3 contents of 34 wt%, whereas quench microphenocrysts have approximately 8 wt% Al_2O_3, and the most rapidly cooled spherulites have 13 wt% Al_2O_3. This increased incorporation of Al in the pyroxene with more rapid cooling rates has been demonstrated experimentally by Walker *et al.* (1978). Similar aluminous clinopyroxene grains have been described from the Gorgona komatiites (Echeverria, 1980; Dietrich *et al.*, 1981) and the Agrilia Formation of the Othris ophiolite (Cameron *et al.*, 1980), although unlike these occurrences, the Al in the King Island clinopyroxenes is dominantly octahedrally co-ordinated.

Unlike the pyroxene, chromite in the picrite flows is uniform in composition (Table 2). The Cr/(Cr + Al)

Table 1

Selected individual analyses and structural formulae (0=6) of clinopyroxene grains from picrite sequence lavas.

	Thin flows		Thick flows					Hyaloclastite		Breccia
Analysis No.	1	2	3	4	5	6	7	8	9	10
Sample No.	R15726		R15700	R33008	R15702		R33009	R33010	R15719	R33011
SiO_2 (wt%)	50.15	47.02	50.39	49.54	44.38	46.37	46.74	51.18	52.12	50.31
TiO_2	0.31	0.32	0.39	0.23	0.62	0.40	0.40	0.34	0.24	0.41
Al_2O_3	3.95	8.60	3.88	6.22	12.87	11.50	10.80	3.11	3.10	5.65
FeO*	8.98	6.35	6.27	4.58	9.97	7.38	9.15	9.05	6.14	10.82
MnO	0.24	0.14	0.21	0.12	0.17	0.17	0.19	0.29	0.18	0.37
MgO	15.83	13.98	16.43	15.75	10.32	11.67	15.31	16.90	16.53	13.61
CaO	19.44	21.90	21.14	22.45	24.19	21.65	16.60	17.99	20.82	17.62
Na_2O	0.25	0.13	0.18	0.14	0.29	0.36	0.21	0.23	0.19	0.25
Cr_2O_3	0.42	0.50	0.16	0.44	0.21	0.15	0.28	0.13	0.25	0.11
NiO	0.05	0.19	0.07	0.10	0.15	0.15	0.05	0.07	nd	nd
Total	99.62	99.13	99.12	99.57	100.17	99.80	99.73	99.29	99.57	99.15
Si	1.872	1.759	1.875	1.828	1.668	1.726	1.729	1.906	1.921	1.884
Ti	0.009	0.009	0.011	0.006	0.017	0.011	0.011	0.010	0.007	0.012
Al^{VI}	0.128	0.241	0.125	0.172	0.332	0.274	0.271	0.094	0.079	0.116
Al^{IV}	0.046	0.138	0.045	0.098	0.238	0.230	0.200	0.042	0.055	0.133
Fe	0.280	0.199	0.195	0.141	0.313	0.230	0.283	0.282	0.189	0.339
Mn	0.008	0.005	0.007	0.004	0.005	0.005	0.006	0.009	0.006	0.012
Mg	0.881	0.780	0.911	0.866	0.578	0.647	0.845	0.938	0.908	0.760
Ca	0.778	0.878	0.843	0.887	0.853	0.863	0.658	0.718	0.822	0.707
Na	0.018	0.009	0.013	0.010	0.021	0.026	0.015	0.016	0.014	0.018
Cr	0.013	0.015	0.005	0.013	0.006	0.005	0.008	0.004	0.007	0.003
Ni	0.001	0.006	0.002	0.003	0.005	0.005	0.001	0.002	-	-
ΣCAT	4.034	4.039	4.032	4.028	4.036	4.002	4.027	4.021	4.008	3.984
Wo	40.0	47.2	43.1	46.7	48.8	49.5	36.7	36.9	42.7	38.9
En	45.2	41.9	46.6	45.6	33.0	37.1	47.1	48.2	47.2	41.8
Fs	14.8	10.9	10.3	7.6	18.2	13.4	16.2	14.9	10.1	19.3
$Mg/Mg + Fe^{2+}$	0.76	0.80	0.82	0.86	0.65	0.74	0.75	0.77	0.83	0.69

* Total Fe as FeO; n.d. below 0.005% detection limit of EMP. Textures of samples are: Analysis No. 1, 2 microphenocrysts; 3, 4 granular pyroxene; 5 plumose textured pyroxene; 6 microphenocryst; 7 spherulitic pyroxene; 8, 9 pyroxene grains; 10 spherulitic pyroxene.

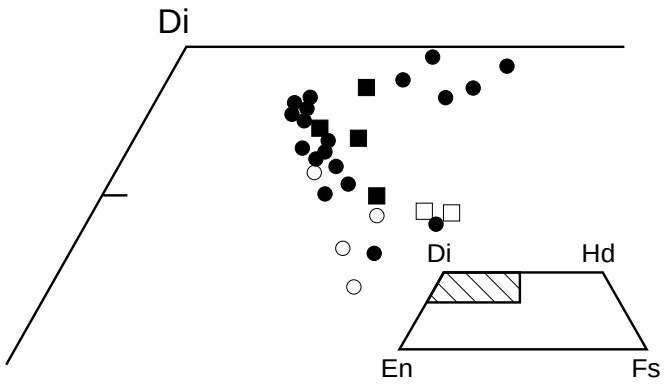

Figure 10

Pyroxene quadrilateral showing the composition of clinopyroxenes from the picrites. Samples are:

- *closed circles, thick flows;*
- *open circles, hyaloclastites;*
- *closed squares, thin flows;*
- *open squares, breccias.*

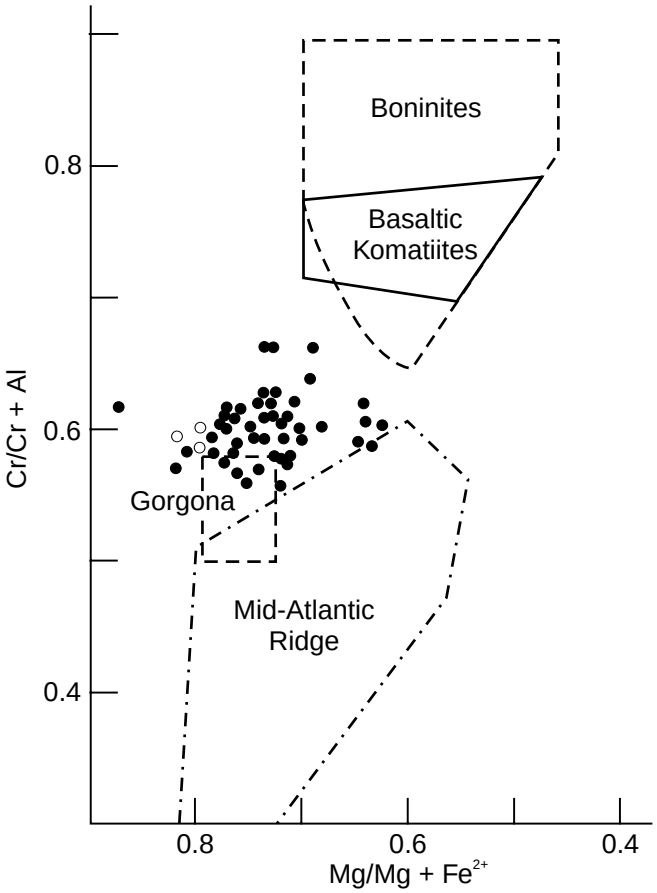

Figure 11

Chrome spinel compositions expressed in terms of Cr/Cr + Al and –Mg/Mg + Fe^{2+}. Samples are:

- *filled circles, picritic flows, breccias, pillows and hyaloclastites;*
- *open circles, picritic cumulate dykes.*

Fields of spinel compositions from other locations are shown:

- *boninites from the Western Pacific and Cape Vogel, Troodos and Othris ophilitic volcanics (Cameron* et al.*, 1979, 1980);*
- *Gorgona komatiites (Dietrich* et al.*, 1981, Echeverria, 1980); and*
- *Mid-Atlantic Ridge (Dick and Bryan, 1979).*

values (fig. 11) are particularly constant and similar to chromites in Gorgona komatiite samples, but quite unlike spinel grains from texturally similar rocks, such as Archaean komatiite and the Othris and Troodos ophiolitic basalt flows. The Cr/(Cr + Al) values also fall within the range of chromite in spinel lherzolite and harzburgite suggested to be residues from melts that have produced tholeiitic liquids (Dick, 1977). The Fe^{3+} /(Fe^{3+} + Cr + Al) values range from 0.04 to 0.19, indicating variable oxygen fugacity of the magma (Fisk and Bence, 1980).

Upper Tholeiite Sequence

Both the porphyritic and non-porphyritic flows of the upper tholeiite sequence consist of albitised plagioclase and calcic clinopyroxene (fig. 12*a*). Fresh labradorite is present in some of the comagmatic dykes intruding the picrite and siltstone successions. The upper tholeiite flows are quite altered in places with the development of actinolite overgrowths, probably due to the proximity of the granitic intrusions. Parts of the underlying picrite and lower tholeiite sequences are also progressively altered towards the contact aureole.

The non-porphyritic flows are vesicular and consist of glomerocrysts of idiomorphic albite (1–1.5 mm in length), zoned sericitised plagioclase, and smaller subhedral augite grains. The groundmass consists of fine-grained interlocking plagioclase laths with interstitial augite, abundant chlorite and accessory epidote, ilmenite and actinolite. Epidote, chlorite and quartz commonly infill vesicles. The porphyritic flows have similar mineralogy, but contain large zoned, completely albitised and partially sericitised plagioclase grains (up to 6 mm across) and chrome diopside phenocrysts (1.5–2 mm long) in a highly altered groundmass of plagioclase, pyroxene, chlorite and epidote.

Tholeiite dykes associated with the upper volcanic sequence are of both porphyritic and non-porphyritic varieties, similar to the flows. The porphyritic dykes consist of sericitised plagioclase phenocrysts set in a medium-grained intergranular groundmass of plagioclase laths and sub-idiomorphic augite. The non-porphyritic dykes have various textures, including coarse-grained ophitic to subophitic varieties, with large augite plates pierced by albite, with accessory sphene and ilmenite. Vesicular varieties, composed of medium-grained interlocking plagioclase laths with interstitial augite, skeletal magnetite, sphene and ilmenite, are also present. Minor, highly-altered dykes with albite glomerocrysts in a chloritic matrix also occur. Intergranular textured dykes consist of fresh labradorite and clinopyroxene. The clinopyroxene shows considerable variability in composition, even within the one dyke, and varies from augite to subcalcic augite and ferroaugite (fig. 12*a*). Clinopyroxenes from some of the ophitic dykes have high TiO_2 contents (1.6–1.9 wt%), typical of alkaline rocks (Nisbet and Pearce, 1977), although the host rocks are tholeiitic. Such features may be a function of cooling rate, as described by Coish and Taylor (1979).

Volcaniclastic conglomerate interbedded with the tholeiitic flows contains volcanic detritus, including lithic fragments of the porphyritic and non-porphyritic lavas with which they are associated. Other tholeiitic lithic fragments include ophitic-textured albite and augite varieties (fig. 12*b*) and fine-grained interlocking plagioclase microphenocrysts with interstitial clinopyroxene, similar to the lower tholeiite massive and pillow basalt flows, respectively. Minor dacitic lithic fragments, similar to those in the basal tuff of the lower tholeiite sequence, are present, as are augite grains (fig.12*b*). No picritic fragments were observed.

Table 2

Selected individual analyses and structural formulae (0=32) of chromite grains from the picrite sequence lavas

	Breccia		Thin Flows		Thick flows	Hyalo-clastite	Pillow lavas		Dykes	
Analysis No.	1	2	3	4	5	6	7	8	9	10
Sample No.	R15693	R33012	R15723	R15726	R33013	R15733	R15731	R33014	R33015	R33016
TiO_2 wt%	n.d.	0.15	0.14	0.19	0.18	0.13	0.20	0.17	0.17	0.24
Al_2O_3	20.34	21.16	19.88	21.48	20.79	17.27	20.75	19.31	23.72	20.90
Cr_2O_3	46.66	46.05	46.44	47.99	48.01	46.49	49.11	47.45	45.15	48.47
Fe_2O_3*	6.18	5.13	6.25	3.39	3.75	9.50	3.02	5.85	4.15	4.16
FeO	9.91	10.89	10.02	8.69	10.91	11.68	10.57	10.36	9.68	9.34
MnO	0.49	0.13	0.72	n.d.	n.d.	0.07	0.07	0.07	n.d.	0.05
MgO	16.08	15.46	15.67	17.32	15.73	14.90	16.05	15.77	16.90	16.86
CaO	n.d.	n.d.	n.d.	0.05	n.d.	0.07	n.d.	0.16	n.d.	n.d.
NiO	0.10	0.23	0.21	n.d.	0.20	0.19	0.25	0.18	0.18	0.18
Total	99.76	99.20	99.33	99.11	99.57	100.05	100.02	99.32	99.95	100.20
Ti	-	0.027	0.026	0.035	0.033	0.034	0.036	0.031	0.030	0.043
Al	5.855	6.112	5.765	6.130	5.986	5.066	5.944	5.610	6.679	5.942
Cr	9.010	8.922	9.034	9.188	9.272	9.090	9.436	9.247	8.528	9.243
Fe^{3+}	1.135	0.945	1.158	0.617	0.689	1.779	0.552	1.085	0.747	0.755
Fe^{2+}	2.025	2.232	2.062	1.760	2.228	2.432	2.148	2.135	1.935	1.884
Mn	0.101	0.026	0.150	-	-	0.014	0.015	0.015	-	0.010
Mg	5.854	5.648	5.747	6.253	5.730	5.527	5.813	5.794	6.020	6.061
Ca	-	-	-	0.012	-	0.019	-	0.043	-	-
Ni	0.020	0.046	0.042	-	0.039	0.038	0.049	0.035	0.035	0.034
Cr/Cr+Al	0.606	0.593	0.610	0.600	0.608	0.642	0.614	0.622	0.561	0.609
$Mg/Mg + Fe^{2+}$	0.743	0.717	0.736	0.780	0.720	0.694	0.730	0.731	0.757	0.763
$Fe^{3+}/Fe^{3+} + Cr + Al$	0.071	0.059	0.073	0.039	0.043	0.112	0.035	0.068	0.047	0.047

* Fe_2O_3 calculated assuming stoichiometry; n.d. below 0.05% detection limit of EMP.

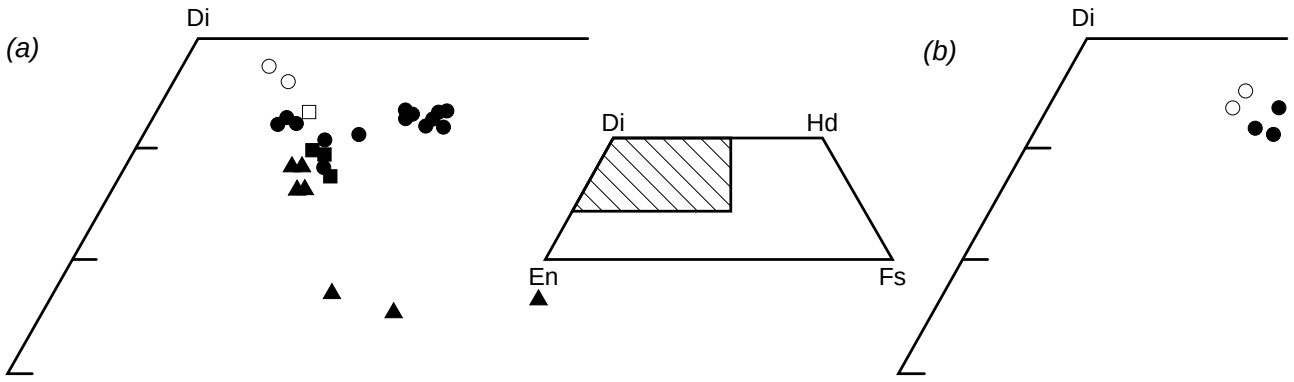

Figure 12

Pyroxene quadrilaterals showing the compositions of clinopyroxenes from the upper tholeiitic sequence.

(a) Clinopyroxenes from non-porphyritic (closed symbols) and porphyritic flows and dykes. Samples are: closed squares, non-porphyritic flows; closed circles, non-porphyritic subophitic-ophitic dykes; closed triangles, non-porphyritic intergranular dykes; open circles, porphyritic flow; open squares, porphyritic dykes.

(b) Volcaniclastic conglomerate pyroxene grains (open circles) and lithic fragments (closed circles).

CHEMISTRY OF THE VOLCANIC SEQUENCES

Alteration

Mineral assemblages described in the previous section indicate that the basalt flows have suffered some alteration, and that the present chemical composition may not be entirely primary. The southeast King Island coast sequence does not appear to have been subjected to significant regional metamorphism, and the alteration is considered to have resulted mainly from reaction with seawater.

The interpretation of the geochemistry of the volcanic sequences is biassed towards the rare earth elements (REE) and high field strength (HFS) minor and trace elements, as these show the greatest resistance to post-magmatic alteration processes (Pearce, 1975; Coish, 1977; Condie *et al*., 1977; Pearce and Norry, 1979; Menzies *et al*., 1979; Saunders *et al*., 1980). Whereas the REE have been shown to be mobile under some circumstances (Frey *et al*., 1974; Wood *et al*., 1976; Menzies e*t al*., 1979; Furnes, 1978; Ludden and Thompson, 1978; 1979; Hellman *et al*., 1979), similar REE contents in fresh and altered volcanic rocks from Troodos (Smewing and Potts, 1976) and in basalts and associated volcanogenic sediments from the Indian Ocean (Fleet *et al*., 1976) indicate REE immobility.

The consistency of chondrite-normalised REE plots of related volcanic samples (fig. 13, 14) suggests that the rocks represent original igneous patterns, and that REE patterns can be used as a basis for elucidating primary magmatic characteristics. This premise has been used by other workers in the interpretation of REE contents of altered volcanic rocks from Troodos (Kay and Senechal, 1976), and Archaean (Sun and Nesbitt, 1978; Jahn and Sun, 1979) and Ordovician (Loeschke and Schock, 1980) greenstone belts.

Lower Tholeiite Sequence

Chemical analyses of massive and pillow basalt samples from the lower tholeiite sequence are given in Table 3. Both the pillow and massive basalt samples are characterised by low TiO_2 contents (0.42 to 0.76 wt%) and are tholeiitic in nature, as indicated by trends on a FeO^t versus FeO^t/MgO plot (Miyashiro, 1974), and by their ol and hy normative characteristics. Some massive basalt samples (analyses 7 and 8, Table 3) and all the pillow basalt samples are particularly uniform in both major and trace element composition, whereas other massive basalt samples (analyses 5 and 6, Table 3) have higher MgO contents and correspondingly lower incompatible trace elements. All the lower tholeiite sequence basalt samples are characterised by low Zr (Table 3), except two samples from minor flows in the siltstone sequence underlying the main mass of the tholeiite sequence. These samples have some chemical similarities to some of the upper tholeiite sequence dykes, but field relationships suggest that the samples come from flows associated with the first tholeiitic volcanic phase.

The CaO/Al_2O_3 values of the lower tholeiite sequence range from 0.51 to 0.74, with smaller values for lower Mg-numbers. This suggests clinopyroxene fractionation was important in their genesis. Similarly, Cr and Ni contents vary systematically with Mg-numbers, indicative of clinopyroxene and/or olivine control. Chondrite-normalised REE patterns for both the massive and pillow basalts (fig. 13) are parallel and show LREE enrichment and slight negative Eu anomalies. The latter feature is probably inherent from shallow-level fractional crystallisation of plagioclase. The parallel nature of the patterns reflects a common source for all samples of this sequence. The lower total REE abundances in the more magnesian samples, and the nature of the REE patterns, suggests that the magma was modified by fractionation of clinopyroxene and plagioclase, consistent with the modal mineralogy.

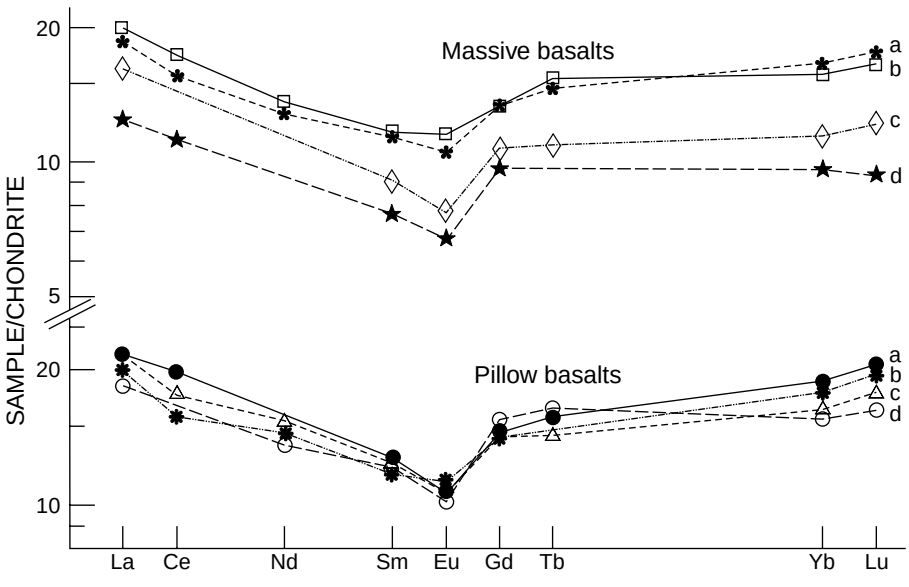

Figure 13

Chondrite normalised REE patterns for the lower tholeiitic massive basalts and pillows.

Chondrite values from Sun and Hanson (1975).

Table 3

Chemical analyses of the lower tholeiite pillow and massive basalt sequence.

	Pillow Basalts				Massive Basalts			
Analysis No.	1	2	3	4	5	6	7	8
Sample No.	R15737*	R33028	R15735*	R33006	R15705*	R15714*	R15668*	R15666*
SiO_2 wt%	51.49	53.34	49.98	50.64	50.76	50.67	51.32	51.54
TiO_2	0.72	0.66	0.73	0.76	0.42	0.46	0.74	0.65
Al_2O_3	12.41	13.44	13.14	12.91	14.77	14.67	13.01	12.73
Fe_2O_3	4.88	12.59+	4.15	14.68+	3.95	2.44	5.33	5.08
FeO	8.74	-	9.84	-	5.81	7.22	8.21	9.35
MnO	0.22	0.24	0.21	0.22	0.17	0.17	0.23	0.21
MgO	6.02	5.40	5.86	6.04	8.41	8.73	5.84	6.18
CaO	11.18	6.81	7.46	6.23	10.99	8.74	7.62	7.43
Na_2O	3.74	5.52	5.54	4.90	2.87	4.29	5.51	4.10
K_2O	0.08	0.05	0.08	0.08	1.27	0.17	0.19	0.20
P_2O_5	0.09	0.08	0.08	0.09	0.06	0.06	0.08	0.08
LOI	1.14	1.30	1.84	1.56	1.28	1.40	2.08	1.01
Total	100.71	99.43	98.91	98.11	100.76	99.02	100.16	98.56
Mg No.	45	46	43	45	62	62	44	44
Rb ppm	n.d.	5	3	4	52	5	4	5
Ba	68	45	53	50	440	146	268	82
Th	1.72	n.d.	n.d.	2.16	n.d.	n.d.	1.07	1.70
Ta	0.14	0.14	0.15	0.21	n.d.	0.31	0.21	0.32
Sr	98	116	37	33	135	156	167	89
Hf	1.41	1.18	1.60	1.69	0.81	1.30	1.30	1.48
Zr	51	45	51	43	33	42	48	45
Y	35	27	40	28	19	24	36	35
Sc	50	46	53	49	47	49	50	50
Ni	97	210	132	44	146	121	53	47
Co	50	46	55	52	39	45	47	53
Cr	26	29	42	19	511	417	28	35
V		364		409				
Cu	118	71	132	71	52	83	111	105
Zn	88	66	101	97	58	73	126	106
S	320	600	960	1230	280	240	680	1800
La	6.22	5.79	6.73	6.82	3.94	5.04	6.28	5.91
Ce	12.75		16.16	14.14	9.02	13.54	14.08	12.73
Nd	8.69	8.14		9.20		8.94	8.11	7.64
Sm	2.26	2.35	2.48	2.42	1.47	1.74	2.24	2.22
Eu	0.80	0.73	0.76	0.77	0.48	0.56	0.83	0.76
Gd	3.67	4.06	3.82	3.63	2.52	2.79	3.41	3.44
Tb	-	0.81	0.77	0.69	-	0.53	0.75	0.72
Yb	3.68	3.25	3.95	3.36	2.01	2.31	3.23	3.38
Lu	0.63	0.52	0.67	0.58	0.30	0.39	0.53	0.56

Sample No. = Registered Sample numbers in the Department of Geology, University of Melbourne Collection.
Mg No. = Molecular proportions 100 Mg/Mg + Fe^{2+}; n.d. = below detection limit; + = Total FeO as Fe_2O_3.

Major and trace elements determined by XRF analysis on fused glass discs according to the method of Haukka and Thomas (1977) and Thomas and Haukka (1978), analyst M. Haukka. * = Major elements determined on fused glass discs and trace elements on pressed powder pellets according to the method of Norrish and Hutton (1969) and Norrish and Chappell (1967), analyst HMW. All XRF analyses performed on a Seimens sequential SRS-1 X-ray fluorescence spectrometer. REE, Hr, Th, Ta determined by instrumental neutron activation analysis after the method of Jacobs *et al*. (1977). Rock powder samples were countered three times after irradiation; 6–9 days for Nd, Sm, Eu (low energy photon detector, LEPD) and La, Yb, Lu (GeLi detector); 70 days for Ce (LEPD) and Tb, Hf, Th, Ta (GeLi); and 6 months for Gd (LEPD), analyst HMW. All analyses performed at the Department of Geology, University of Melbourne.

Table 4

Representative chemical analyses of the picrite sequence.

	Thick Flows		Pillow	Thin flows			Breccia	Hyaloclastite
Analysis No.	1	2	3	4	5	6	7	8
Sample No.	R15702*	R33032	R33033	R15732*	R15734*	R33031	R33027	R33041
SiO_2 wt%	46.24	43.67	46.41	47.52	42.47	50.86	42.96	48.25
TiO_2	0.22	0.33	0.21	0.26	0.29	0.22	0.26	0.25
Al_2O_3	8.46	10.36	7.81	8.47	11.57	5.41	11.17	8.59
Fe_2O_3	8.08+	9.15+	8.37+	2.35	2.65	9.21+	10.17+	9.30+
FeO				6.94	8.36			
MnO	0.17	0.17	0.15	0.17	0.19	0.22	0.14	0.28
MgO	20.34	20.22	21.21	20.58	20.13	17.99	21.32	16.84
CaO	11.62	10.77	9.64	9.85	8.01	12.15	6.48	11.98
Na_2O	0.31	0.22	0.19	0.35	0.32	0.25	0.24	0.56
K_2O	0.01	0.01	0.01	0.34	0.33	0.02	0.02	0.14
P_2O_5	0.02	0.02	0.02	0.03	0.03	0.02	0.02	0.03
LOI	3.98	4.66	4.61	3.06	5.27	2.75	6.72	3.09
Total	99.45	99.58	98.54	99.92	99.62	99.10	99.50	99.31
Mg No.	83	81	83	80	77	79	81	78
Rb ppm	3	2	<1	10	8	3	<1	5
Ba	17	16	14	375	541	17	11	125
Sr	3	4	4	11	9	6	17	19
Zr	11	15	10	6	8	13	12	14
Y	7	12	7	12	15	7	10	6
Sc	33	38	28	38	38	31	34	22
Ni	772	738	1213	769	873	566	893	786
Co	58	76	77	73	81	62	83	63
Cr	1650	1627	2347	2610	2460	1710	2440	1701
Cu	13	11	33	47	44	37	89	21
Zn	47	49	42	56	67	60	53	50
S	20	22	35	8#	63#	53	54	58
La	0.18	0.17	0.26	0.21	0.29	0.29	0.37	1.25
Ce	0.22	0.47	0.62	0.49	0.81	0.66	0.75	2.77
Nd	0.70	0.80	0.69	0.62	1.00	0.63	0.86	1.91
Sm	0.44	0.62	0.38	0.43	0.55	0.45	0.52	0.65
Eu	0.21	0.31	0.18	0.18	0.17	0.18	0.31	0.31
Gd	0.95	1.28	0.72	0.89	1.38	0.91	1.06	0.97
Tb	0.20	0.30	0.18	0.22	0.29	0.21	0.26	0.20
Ho	0.47	0.52	0.32	0.49	0.49	0.40	0.48	0.39
Tm	0.17	0.20	0.13	0.19	0.22	0.17	0.18	0.16
Yb	1.46	1.79	1.26	1.58	1.69	1.41	1.82	1.25
Lu	0.23	0.28	0.21	0.27	0.27	0.22	0.30	0.20

Mg No. = Molecular proportions 100 Mg/Mg + Fe^{2+}; + = Total Fe as Fe_2O_3; * = Trace elements determined on pressed powder pellets; # = S determined by Leco Automatic Sulphur Titrator. REE determined by radiochemical neutron activation according to the method by Bishop and Hughes (1984).

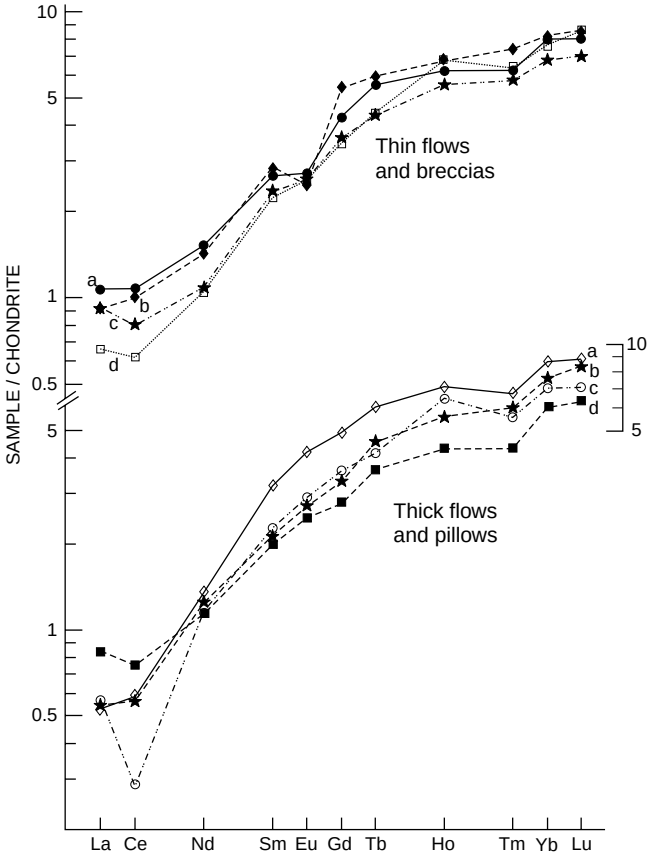

Figure 14

Chondrite-normalised REE patterns for the picritic thin flows and breccias, and pillows and thick flows.

The low contents of TiO_2 and Zr, and the LREE-enriched nature of the massive and pillow basalts, reflect mantle source characteristics. The low concentration of HFS elements suggests partial melting of a depleted mantle source, with the addition of a LREE-enriched, but Ti-poor, component. The generation of such an enriching component probably involves the retention of Ti and Zr in the residue, possibly in minor minerals, as described by Green (1980). Similar enriching events have been proposed by several workers to explain the composition of boninite (Nesbitt and Sun, 1980; Hickey and Frey, 1979; Jenner, 1981), island arc tholeiite (Perfit *et al.*, 1980; Foden and Varne, 1980), and P-type Mid Ocean Ridge Basalt (Sun *et al.*, 1979).

Some massive basalt samples from the base of the lower tholeiite sequence have relatively higher Zr, TiO_2, and LREE contents than the majority of the samples from the massive and pillow basalt units. Such compositional differences suggest a heterogeneous mantle source, with irregularly distributed volumes of variable enrichment.

Picrite Sequence

Chemical analyses of representative samples of picrite units are given in Table 4. Magnesia content ranges from 8–23 wt% with the majority of samples containing between 16 and 21 wt% MgO. Mg-numbers are high, ranging from 63 to 84. Such high Mg-numbers are characteristic of primitive magmas, but low abundances of incompatible elements, particularly the low and constant TiO_2 content and severe LREE depletion (fig. 14), reflect a refractory mantle source.

The chemical composition of the picrite units is remarkably uniform despite the variation in morphology, which is thought to have resulted from different degrees of physical interaction with seawater. The uniformity of TiO_2 and the correspondence of MgO contents with modal amounts of olivine and clinopyroxene indicates that abundances of these elements are probably close to being primary, with the MgO content of the pseudomorphed olivine retained in the secondary minerals. Metasomatic addition of MgO from seawater to the picritic lavas, as suggested by experimental work with high rock/water ratios (Bischoff and Dickson, 1975; Janecky, 1979; Pohl and Dickson, 1979), has apparently not occurred.

Apparent LREE enrichment due to seawater alteration (Frey *et al.*, 1974; Menzies *et al.*, 1977; Ludden and Thompson, 1978, 1979; Hellman *et al.*, 1979) is shown by the REE contents of some of the hyaloclastite samples subjected to greater submarine weathering than the less fragmental picrite flows. Comparison of Figure 14 with Figure 15 shows that the hyaloclastite HREE content is the same as the less fragmental rocks, but that the hyaloclastite units are enriched in LREE. Mobility of Eu in basalt, with the development of both positive and negative anomalies due to alteration, has been reported by Sun and Nesbitt (1978) and Jahn and Sun (1979). The consistency of the negative Eu anomalies in the picritic thin flows and breccia samples suggests that this may be a magmatic rather than alteration feature.

It is suggested that the LREE depletion in the picrite samples reflects magmatic characteristics, and if modified by secondary processes, represents minimum magmatic patterns. This strengthens the contention that the picrite sequence was derived from a refractory mantle source.

The sympathetic variation of Cr, Ni and Co with Mg-number and the original phenocryst mineralogy

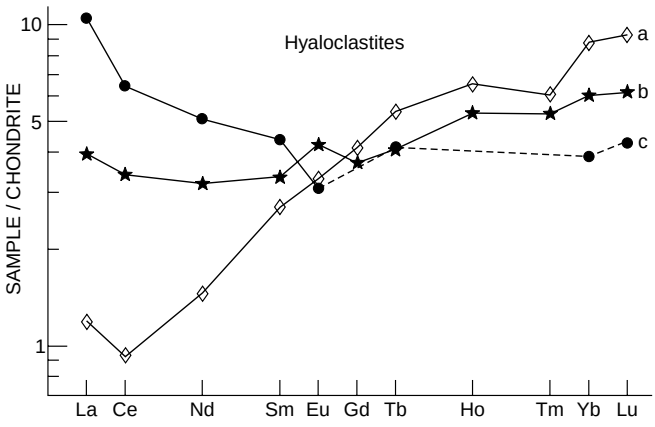

Figure 15

Chondrite-normalised REE patterns for the picritic hyaloclastites.

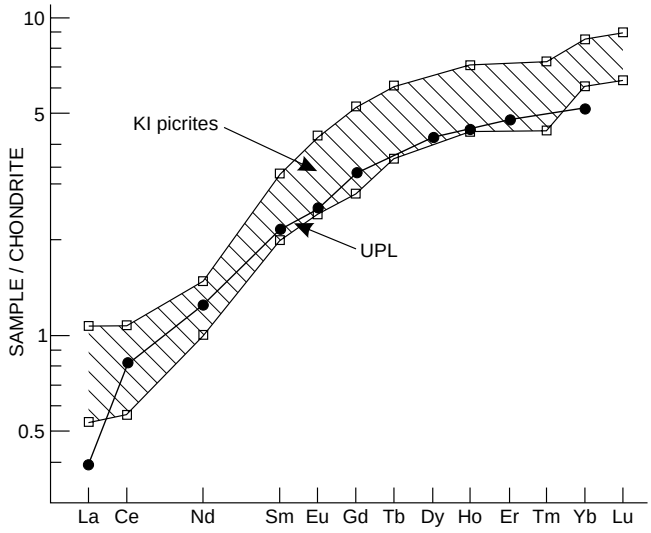

Figure 16

Chondrite-normalised REE patterns showing the range for the King Island picrites and an Upper Pillow Lava sample for Troodos (Kay and Senechal, 1976).

suggests that the chemical variation in the picrite sequence can be explained by olivine and minor amounts of clinopyroxene fractionation or crystal accumulation. The parallel REE patterns (fig. 14) are consistent with this proposed fractionation. Slight negative Eu anomalies in some of the picritic REE patterns suggest that minor shallow-level plagioclase fractionation may have formed an integral part of the system.

The King Island picrite sequence has some of the characteristics of other high-magnesian, low-alkali volcanic rocks described in the literature, but has no direct analogue in any one occurrence. Rather, the picrites exhibit a combination of characteristic features of several separate examples. The King Island picrite sequence is more depleted in incompatible elements than texturally similar rocks from Gorgona (Echeverria, 1980; Dietrich *et al*., 1981), Cape Smith (Schwarz and Fujiwara, 1977), and Baffin Island–Svartenhuk (Clarke, 1970; O'Nions and Clarke, 1972). Compared with Archaean komatiites (Sun and Nesbitt, 1978) of similar major element composition, the picrite sequence is more depleted in LREE. Average Ti/Zr and Zr/Y ratios of 160 and 1, respectively, for the picrite sequence are quite different from the chondritic values characteristic of komatiite (Nesbitt and Sun, 1980). Olivine and clinopyroxene phyric basalt samples from the Upper Pillow Lava sequence at Troodos (Smewing *et al*., 1975; Smewing and Potts, 1976) have incompatible element contents, particularly LREE (fig. 16), similar to the picrite units. However the King Island picrite sequence contains considerably less refractory chromite (fig. 11) than volcanic rocks from Troodos (Cameron *et al*., 1979, 1980).

The King Island picrite sequence is also clearly unlike boninitic lavas from Bonin Island (Shiraki and Kuroda, 1977; Kuroda and Shiraki, 1975), the Mariana Trench (Dietrich *et al*., 1978), Cape Vogel (Jenner, 1981), and Tasmania (Brown and Jenner, 1989), which have high SiO_2 contents, LREE enrichment, and a characteristic dish-shaped chondrite-normalised REE pattern.

Upper Tholeiite Sequence

Only preliminary work has been done on the upper tholeiite units, and the compositional data presented may not be fully representative of the sequence as a whole. Rocks of the upper tholeiite sequence are clearly chemically distinct from the lower tholeiite sequence.

Chemical analyses of some porphyritic and non-porphyritic flows and dykes are given in Table 5. These define a tholeiitic trend on a FeO^t versus FeO^t/MgO plot (after Miyashiro, 1974). The aphyric flows and some of the dykes contain over 14% Fe_2O_3 (as total Fe), and probably represent differentiates of the porphyritic lavas following an Fe-enrichment trend. The trace element abundances of the upper tholeiite sequence show no depletion in incompatible elements, which is quite unlike the lower tholeiite sequence.

The chrondite-normalised REE patterns (fig. 17) from samples of the upper tholeiite sequence show a depletion in HREE for the porphyritic flows and dykes and the non-porphyritic flows. This depletion of HREE suggests retention of garnet in the residue. High Al_2O_3 and low Y contents are consistent with residual garnet, and low concentrations of Sc and Y suggest clinopyroxene may also have been a residual phase. The non-porphyritic dykes have near-parallel REE patterns with lower total REE abundances in the more magnesian samples. The HREE patterns from these dykes are flat compared with the associated flows and

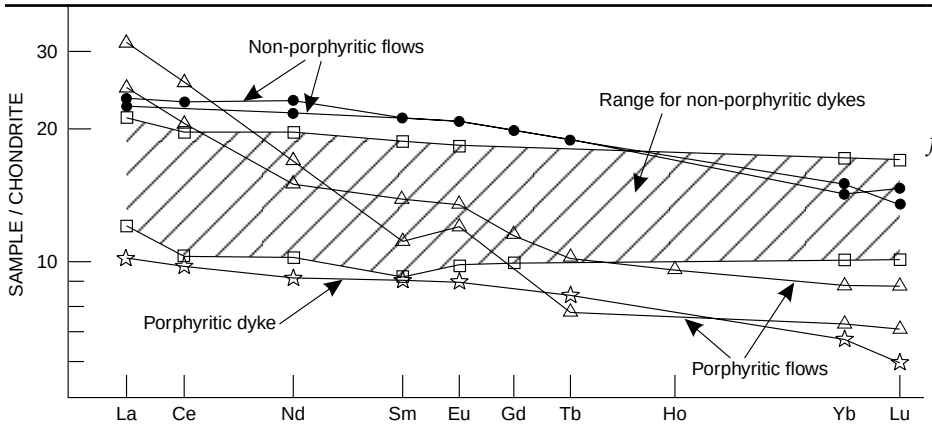

Figure 17

Chondrite-normalised REE patterns for the upper tholeiitic porphyritic and non-porphyritic flows and dykes.

Table 5

Representative chemical analyses of the upper tholeiite sequence.

	Non-porphyritic		Porphyritic	
	Flow	Dyke	Flow	Dyke
Analysis No.	1	2	3	4
Sample No.	R33029	R33022	R33025	R15697
SiO_2	49.01	47.34	45.63	45.19
TiO_2	1.72	0.78	0.82	0.73
Al_2O_3	14.22	14.87	17.32	19.26
Fe_2O_3*	14.34	12.12	9.27	8.22
MnO	0.20	0.15	0.15	0.13
MgO	6.49	8.03	9.05	8.02
CaO	6.42	9.67	10.17	9.88
Na_2O	4.80	2.97	2.15	2.39
K_2O	0.25	0.98	0.89	1.61
P_2O_5	0.15	0.09	0.10	0.07
LOI	1.84	2.31	3.64	3.15
Total	99.44	99.31	99.19	98.65
Mg No.	47	57	66	66
Rb ppm	13	55	29	61
Ba	118	170	378	665
Sr	165	735	182	700
Zr	85	60	40	52
Y	24	20	9	14
Sc	40	43	34	32
Ni	79	134	162	199
Co	56	55	40	65
Cr	144	282	398	492
V	379	323	202	197
Cu	110	130	52	58
Zn	105	74	51	47
S	60	70	54	145
La	7.55	3.95	10.12	3.36
Ce	15.58	8.45	20.58	8.58
Nd	13.59	6.06	10.51	5.69
Sm	4.03	1.76	2.14	1.77
Eu	1.50	0.70	0.87	0.66
Gd	5.08	2.56	-	-
Tb	0.91	-	0.37	0.48
Yb	2.98	2.02	1.45	1.32
Lu	0.42	0.31	0.22	0.18

Mg No. = molecular proportions $100Mg/Mg + Fe^{2+}$; n.d. = below detection limit; * = Total Fe as Fe_2O_3.

dykes. It is suggested that low pressure fractionation of ubiquitous sphene may be responsible for the enrichment in HREE from the parental HREE depleted liquid.

One anomalous sample (e.g. analysis 4, Table 5) is LREE enriched. This sample contains magnesian chrome-diopside phenocrysts and minor chrome-spinel, suggesting possible mixing with picritic magma. However such a process would result in lower total REE contents, particularly LREE. The LREE enrichment may be due to alteration, but since only one sample of this type has been analysed, its petrogenesis can not be resolved at this time.

Preliminary geochemical data for the upper tholeiite sequence indicate that these rocks may have been derived from low percentage partial melting of relatively fertile mantle, with the separation of their primary magma before garnet and clinopyroxene were exhausted in the mantle source.

Miscellaneous Dykes

Lamprophyre

A thin lamprophyre dyke (analysis 3, Table 6) cuts across the picrite sequence to the south of Cumberland Creek. This dyke consists of large, fractured olivine phenocrysts (Fo_{86-92}) surrounded by haloes of magnetite granules, kinked biotite (phlogopite?) xenocrysts and salite ($Wo_{41}En_{47}Fs_{12}$) xenocrysts with prominent reaction rims, in a groundmass of titaniferous sodic clinopyroxene, biotite and alkali feldspar. Accessory amounts of ilmenite, apatite, tremolite (alteration?), pyrite and chalcopyrite are present, with patches of carbonate and magnetite granules scattered throughout. Small granulite nodules, similar to the granulite facies rocks found in Eastern Antarctica, are also present (Harley, 1985). These inclusions indicate an older continental basement for eastern King Island, a feature not so far found on the Tasmanian mainland.

Syenite

Several thick augite syenite dykes intrude the lower sedimentary succession and are roughly concordant with the regional north–south trend. The dykes have fine-grained margins, but are generally coarser grained towards the base. Metamorphosed contacts with the host sediments have been observed.

The margins of the dykes consist of small laths of feldspar, some hollow feldspar grains, and minor small clinopyroxene plates in a groundmass of radially-arranged sheaves of feldspar (fig. 18). Medium-grained samples consist dominantly of 0.5 mm long feldspar laths and some larger feldspar grains with interstitial clinopyroxene. The coarse-grained basal varieties are composed of intergranular textured subhedral augite and feldspar plates (up to 5 mm across) with interstitial finer-grained pyroxene, feldspar and quartz. Some samples are vesicular, others contain abundant pyrrhotite. Augite compositions ranges from $Wo_{36}En_{43}Fs_{21}$ to $Wo_{39}En_{51}Fs_{10}$, but grains are often partly or completely pseudomorphed by chlorite. The feldspar may be albite, oligoclase or orthoclase, and is partially altered to sericite. Other secondary minerals include amphibole, tremolite and prehnite.

The syenitic nature of the dykes is indicated by representative chemical analyses of samples from the centre and base of the intrusions (Table 6). Major and trace element variations are consistent with the modal mineralogy. Greater amounts of orthoclase and quartz,

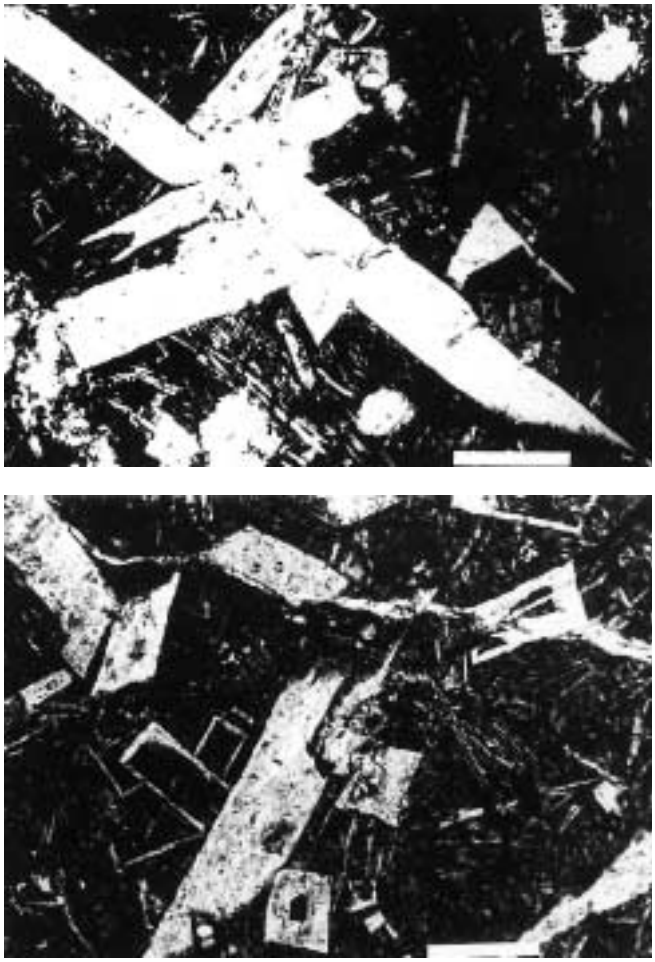

Figure 18

Photomicrographs showing feldspar phenocrysts, including hollow crystals, in a fine feldspar lath groundmass, from the margins of a thick syenite dyke. Scale bar 500 μm.

and less augite and plagioclase, are found towards the base.

The syenitic and lamprophyric intrusions are not related. The trend of the Jurassic–Cretaceous (McDougall and Leggo, 1965; Gleadow and Duddy, 1980) lamprophyre dyke is parallel with the fault system which offsets the north–south trending syenite dykes (fig. 3). This structural constraint, and the presence of metamorphic mineral assemblages in the syenite, indicates that the syenitic dykes are older than the lamprophyric intrusion.

The concordance of the syenitic dykes with the regional trend of the volcano-sedimentary successions suggests a possible genetic relationship. The syenite may have formed by melting of lower crustal material by heat generated from the diapirs producing the voluminous basaltic rocks exposed along the southeast coast. A similar mechanism has been postulated by Cox (1972) to account for alkaline magmatism associated with late stages of crustal rift volcanism in the Karroo Volcanics.

DISCUSSION

The three volcanic associations exposed along the southeast coast of King Island overlie a sedimentary succession of sandstone, siltstone, mixtite and dolomite. The initiation of tholeiitic volcanism was contemporaneous with sedimentation and marked by agglomerate, breccia and tuff units, which include dacitic fragments, followed by outpouring of massive and pillow lavas. Most of the lower tholeiite sequence samples are depleted in Ti and Zr, but enriched in LREE, although some flows less depleted in HFS elements do occur. The overlying picritic pillow lava and tabular flows, and breccia and hyaloclastite units, are characterised by high Mg-numbers and very low incompatible element concentrations, particularly LREE. In contrast, the upper tholeiite sequence samples are not depleted in trace elements and display marked effects of residual garnet and clinopyroxene in the source.

Geological constraints suggest that the setting of the King Island volcano-sedimentary sequence was an intracontinental rift. Indeed, fluid dynamic models (Sparks *et al*., 1980; Huppert and Sparks, 1980) suggest that dense picritic magmas are only likely to reach the surface during periods of continental rifting. Occurrences of some other high-magnesian, low-alkali liquids, such as the Proterozoic Cape Smith basalt succession and those of the Tertiary North Atlantic Province, are also thought to have been erupted in continental rift environments (Schwarz and Fujiwara, 1977; Clarke and Upton, 1971).

Table 6

Bulk rock analyses of augite, syenite and lamprophyre dykes

	Syenite		Lamprophyre
	Centre	Base	
Analysis No.	1	2	3
Sample No.	R33003	R33002	R33001
SiO_2 *(wt%)*	57.05	60.51	34.90
TiO_2	0.62	0.67	2.01
Al_2O_3	14.65	14.92	7.94
Fe_2O_3*	7.26	6.00	11.17
MnO	0.13	0.10	0.19
MgO	6.70	3.42	13.06
CaO	5.25	4.53	12.97
Na_2O	3.20	2.84	1.52
K_2O	2.23	3.44	3.41
P_2O_5	0.12	0.12	1.90
LOI	2.21	2.57	9.39
Total	99.42	99.12	98.41
Rb *(ppm)*	103	98	100
Ba	619	550	2520
Sr	110	213	1640
Zr	127	156	260
Y	28	32	29
Sc	25	23	17
Ni	51	14	435
Co	21	16	63
Cr	125	58	516
V	143	127	168
Cu	19	14	75
Zn	62	66	103
S	100	130	1640

* Total Fe as Fe_2O_3

Although a detailed discussion of the petrogenesis of the volcanic rocks is beyond the scope of this paper, the origin of the tholeiitic and picritic sequences in a probable intracontinental rift setting is relevant.

The lower tholeiite sequence represents the first phase of volcanism initiated by rifting. The chemistry of these tholeiitic rocks indicates that they were produced by partial melting of a depleted mantle source, and enriched by a LREE fraction. The depletion of the source may have been a result of the extraction of a melt associated with earlier dacitic volcanism, represented only by included fragments in tuffs on King Island. The difference in composition of some of the basalts in the lower tholeiite sequence suggests that the enriching phase was generated from irregularly distributed enriched pockets, as described in Hanson (1977), rather than from an enriched layer as in the stratified low-velocity zone model (Green and Liebermann, 1976).

The chemically depleted nature of the tholeiitic sequence, with superimposed incompatible element enrichment, is characteristic of plume-related basalt suites erupted in continental rift environments (Sun *et al*., 1979; Schilling, 1975). Isotopic data for P-type MORB (O'Nions *et al*., 1977) indicate that the rocks were derived from a mantle with a history of long-term depletion and more recent (<300 m.y.) enrichment (Sun *et al*., 1979; Sun, 1980). Isotopic data are not available for the lower tholeiite sequence, but the depleted, with superimposed enriched chemistry, suggests that enrichment, as well as depletion, histories may have been operative as early as the Eocambrian–Cambrian.

The high Mg-numbers of the King Island picrite sequence are characteristic of primitive magmas, but the severe incompatible element depletion indicates that the magmas were derived from a refractory mantle source, rather than by high degree partial melting of mantle pyrolite. The picrites may represent a second-stage melt extracted from a lherzolite diapir, which was the residuum of a previous partial melt of upper mantle pyrolite, as described by Green *et al*. (1979), Duncan and Green (1980), and Jaques and Green (1980). Gold and Pd contents of the picrite samples are similar to precious metal contents of other low-Ti basalt suites (Keays, 1982; Hamilyn *et al*., 1985), also considered to be the product of second-stage melts.

The lower tholeiite sequence and the overlying picritic suite do not appear to be genetically related. The extraction of the LREE-enriched lower tholeiite sequence lavas would not result in a sufficiently refractory residue capable of generating the picrite sequence. The picrite suite, therefore, probably resulted from melting of a mantle source depleted from a previous melting episode not represented on King Island.

It has been argued that other occurrences of high magnesian lavas overlying tholeiitic basalt; such as in Iceland (Wood, 1978, 1981); the Faeroe Island (Schilling and Noe-Nygaard, 1974); Skye (Mattey *et al*. 1977); and the Burin Group, East Newfoundland (Strong and Dostal, 1980) may be genetically related (Wood, 1979; Strong and Dostal, 1980). The authors mentioned have used a dynamic partial melting model (Langmuir *et al*., 1977) to explain the derivation of the high magnesian lavas and the associated tholeiite suites from a single mantle source. However dynamic melting models predict a continuum of compositions between end members and increasingly smaller volumes of sequential melts. Although the occurrences mentioned above do exhibit such compositional variations, the King Island volcanic rocks do not. The second-stage model of Green *et al*. (1979) and Duncan and Green (1980) may therefore be more applicable to the petrogenesis of the King Island picrite suite than the dynamic melting model.

Chemically, the upper tholeiite sequences are non-depleted and represent low-degree partial melts of an upper mantle source. They could not have been derived by fractionation from the underlying, refractory, picritic suite residua, even by complex fractionation schemes, such as periodic refilling of the magma chamber as described by O'Hara (1977) and O'Hara and Matthews (1981).

The volcanic sequences on southeastern King Island are thought to have been generated by variable degrees of partial melting of the upper mantle, similar to the genesis of MORB as described by Wilkinson (1982). The variation in geochemistry of the King Island basaltic suites implies gross compositional heterogeneity in the mantle source region if they were all formed in the same tectonic setting.

The southeast coast sequences have been correlated with sedimentary and volcanic rocks in the Smithton Trough in northwestern Tasmania (Solomon, 1969; Williams, 1978; see Burrett and Martin, 1989 for a review) but the geochemical data presented here indicate that a direct, one-to-one correlation, does not exist.

When comparing the chemistry of the King Island tholeiitic and picritic suites with both published (Brown, 1986; Waldron and Brown, 1986) and unpublished (AVB) data on the tholeiitic rocks from the Smithton Basin there is no direct chemical correlation between any of the suites. The only volcanic rocks within the Smithton Basin which have a similar TiO_2 range to those on King Island occur in the Trowutta area to the south of the Basin. There are, however, significant differences in other elements, especially SiO_2 and Zr (lower); Al_2O_3, MgO, P_2O_5, Cr, and Ni (higher); and REE patterns.

In the Smithton area, rock successions of Eocambrian–Cambrian age unconformably overlie rock successions of Precambrian age. Although the pre-volcanosedimentary rock successions on southeastern King Island are lithologically similar to those in northwestern Tasmania, the latter rocks are structurally far more complex, and no direct comparison can be made between the two areas (see Burrett and Martin, 1989).

Brief descriptions of rocks from the Bowers Group, Antarctica, reported by Jordan (1981), suggest a possible relationship with the King Island sequences. It may be that the King Island sequences are an extension of the Bowers Group, and thus formed as one of a series of *en echelon* troughs in the area now occupied by Victoria, Tasmania and Northern Victoria Land, similar to that suggested by Findlay *et al*. (1991), and are not a linear continuation of the Smithton Trough as concluded by earlier writers.

REFERENCES

ARNDT, N. T.; FRANCIS, D.; HYNES, A. J. 1979. The field characteristics and petrology of Archaean–Proterozoic komatiites. *Canadian Mineralogist* 17:147–163.

ARNDT, N. T.; NALDRETT, A. J.; PYKE, D. R. 1977. Komatiitic and iron-rich tholeiitic lavas of Munro Township, northeast Ontario. *Journal of Petrology* 18:319–369.

BAILLIE, P. W.; SUTHERLAND, F. L. 1992. Devonian lamprophyres from Mt Lyell, western Tasmania. *Papers Proceedings Royal Society Tasmania* 126:19–22.

BALLARD, R. D.; MOORE, J. G. 1977. *Photographic atlas of the Mid-Atlantic Ridge Rift Valley*. Springer-Verlag : New York.

BISCHOFF, J. L.; DICKSON, F. W. 1975. Seawater-basalt interaction at 200°C and 500 bars: Implications for origin of sea-floor heavy-metal deposits and regulation of seawater chemistry. *Earth and Planetary Science Letters* 25:385–397.

BISHOP, J. G.; HUGHES, T. C. 1984. Radiochemical neutron activation analysis determination of rare earth elements in geological materials with ppb sensitivity. *Journal of Radioanalytical and Nuclear Chemistry* 84:213–221.

BLANCHARD, D. P.; RHODES, J. M.; DUNGAN, M. A.; ROGERS, K. V.; DONALDSON, C. H.; BRANNON, J. C.; JACOBS, J. W.; GIBSON, E. K. 1976. The chemistry and petrology of basalts from Leg 37 of the Deep-Sea Drilling Project. *Journal of Geophysical Research* 81:4231–4246.

BROWN, A. V. 1986. Geology of the Dundas–Mt Lindsay–Mt Youngbuck area. *Bulletin Geological Survey Tasmania* 62.

BROWN, A. V.; JENNER, G. A. 1989. Geological setting, petrology and chemistry of Cambrian boninite and low-Ti tholeiite lavas in western Tasmania, *in:* CRAWFORD, A. J. (ed.). *Boninites and related rocks*. Allen and Unwin : London.

BROWN, S. G. 1990. King Island scheelite deposits, *in:* HUGHES, F. E. (ed.). Geology of the Mineral Deposits of Australia and Papua New Guinea. *Monograph Serial Australasian Institute of Mining and Metallurgy* 14:1175–1180.

BURRETT, C. F.; MARTIN, E. L. (ed.). 1989. Geology and mineral resources of Tasmania. *Special Publication Geological Society Australia* 15.

CAMERON, W. E.; NISBET, E. G.; DIETRICH, V. J. 1979. Boninites, komatiites and ophiolitic basalts. *Nature* 280:550–553.

CAMERON, W. E.; NISBET, E. G.; DIETRICH, V. J. 1980. Petrographic dissimilarities between ophiolitic and ocean-floor basalts, *in:* PANAYIOTOU, A. (ed.). *Ophiolites. Proceedings International Ophiolite Symposium, Cyprus, 1979*. 182–192. Ministry of Agriculture and Natural Resources : Cyprus.

CAMPANA, B. 1958. The Flinders Ranges, *in:* GLAESNER, M. F.; PARKIN, L. W. (ed.). The geology of South Australia. *Journal Geological Society Australia* 5:28–45.

CAREY, S. W. 1947. Occurrence of tillite on King Island. *Report Australian and New Zealand Association for the Advancement of Science* 25:349.

CHAPMAN, F. 1912. Notes on a collection of Tertiary limestones and their fossil contents, from King Island. *Memoirs National Museum Melbourne* 4:39–53.

CLARKE, D. B. 1970. Tertiary basalts of Baffin Bay; possible primary magma from the mantle. *Contributions to Mineralogy and Petrology* 25:203–224.

CLARKE, D. B.; UPTON, B. G. J. 1971. Tertiary basalts of Baffin Island; field relations and tectonic setting. *Canadian Journal of Earth Sciences* 8:248–258.

COATS, R. P. 1964. Umberatana Group (new name), *in:* THOMSON, B. P.; *et al.* (ed.). Precambrian rock groups in the Adelaide Geosyncline : A new sub-division. *Quarterly Geological Notes South Australian Geological Survey* 9:7–12.

COATS, R. P. 1971. Regional geology of the Mount Painter Province: Precambrian basement cover — The Adelaide System, *in:* COATS, R. P.; BLISSETT, A. H. (ed.). Regional and economic geology of the Mount Painter Province. *Bulletin South Australia Geological Survey* 43:47–92.

COATS, R. P.; PREISS, W. V. 1980. Stratigraphic and geochronological reinterpretation of Late Proterozoic glaciogenic sequences in the Kimberley Region, Western Australia. *Precambrian Research* 13:181–208.

COISH, R. A. 1977. Ocean floor metamorphism in the Betts Cove Ophiolite, Newfoundland. *Contributions to Mineralogy and Petrology* 60:255–270.

COISH, R. A.; TAYLOR, L. A. 1979. The effects of cooling rate on texture and pyroxene chemistry in DSDP Leg 34 basalt: a microprobe study. *Earth and Planetary Science Letters* 42:389–398.

CONDIE, K. C.; VILJOEN, M. J.; KABLE, E. J. D. 1977. Effects of alteration on element distributions in Archean tholeiites from the Barberton greenstone belt, South Africa. *Contributions to Mineralogy and Petrology* 64:75–89.

COOPER, P. F. 1973. Striated pebbles from the late Precambrian Adelaidean. *Quarterly Geological Notes New South Wales Geological Survey* 11:13–15.

COX, K. G. 1972. The Karroo volcanic cycle. *Journal Geological Society of London* 128:311–336.

CRAWFORD, A. J.; BERRY, R. F. 1992. Tectonic implications of late Proterozoic–early Palaeozoic igneous rock associations in western Tasmania. *Tectonophysics* 214:37-56.

CRAWFORD, A. J.; CAMERON, W. E.; KEAYS, R. R. 1984. The association boninite low-Ti andesite-tholeiite in the Heathcote Greenstone Belt, Victoria; ensimatic setting for the early Lachlan Fold Belt. *Australian Journal of Earth Sciences* 31:161–175.

CRESPIN, I. 1945. Middle Miocene limestones from King Island, Tasmania. *Papers Proceedings Royal Society Tasmania* 1944:15–18.

DANIELSON, M. J. 1975. King Island scheelite deposits, *in:* KNIGHT, C. L. (ed.). Economic geology of Australia and Papua New Guinea. *Monograph Serial Australasian Institute of Mining and Metallurgy* 5:592–598.

DICK, H. J. B. 1977. Partial melting in the Josephine Peridotite 1, the effect on mineral composition and its consequence for geobarometry and geothermometry. *American Journal of Science* 277:801–832.

DICK, H. J. B.; BRYAN, W. D. 1979. Variation of basalt phenocryst mineralogy and rock compositions in DSDP Hole 396B. *Initial Report Deep Sea Drilling Project* 46:215–225.

DIETRICH, V.; EMMERMANN, R.; OBERHÄNSLI, R.; PUCHELT, H. 1978. Geochemistry of basaltic and gabbroic rocks from the West Mariana basin and the Mariana trench. *Earth and Planetary Science Letters* 39:127–144.

DIETRICH, V. J.; GANNSER, A.; SOMMERAUER, J.; CAMERON, W. E. 1981. Palaeogene komatiites from Gorgona Island, East Pacific — A primary magma for ocean floor basalts? *Geochemical Journal* 15:141–161.

DIMROTH, E.; LICHTBLAU, A. P. 1979. Metamorphic evolution of Archean hyaloclastites, Noranda area, Quebec, Canada. Part 1: Comparison of Archean and Cenozoic sea-floor metamorphism. *Canadian Journal of Earth Sciences* 16:1315–1340.

DIMROTH, E.; COUSINEAU, P.; LEDUC, M.; SANSCHAGRIN, Y. 1978. Structure and organization of Archean subaqueous basalt flows, Rouyn–Noranda area, Quebec, Canada. *Canadian Journal of Earth Sciences* 15:902–918.

DONALDSON, C. H. 1976. An experimental investigation of olivine morphology. *Contributions to Mineralogy and Petrology* 57:187–213.

DUNCAN, R. A.; GREEN, D. H. 1980. Role of multistage melting in the formation of oceanic crust. *Geology* 8:22–26.

ECHEVERRIA, L. M. 1980. Tertiary or Mesozoic komatiites from Gorgona Island, Colombia: Field relations and geochemistry. *Contributions to Mineralogy and Petrology* 73:253–266.

FINDLAY, R. H.; BROWN, A. V.; MCCLENAGHAN, M. P. 1991. Confirmation of the correlation between Lower Palaeozoic rocks in western Tasmania and Northern Victoria Land, Antarctica, and a revised tectonic interpretation. *Memorie Della Societa Geologicà Italiana* 46:117–133.

FISK, M. R.; BENCE, A. E. 1980. Experimental crystallization of chrome spinel in FAMOUS basalt 527-1-1. *Earth and Planetary Science Letters* 48:111–123.

FLEET, A. J.; HENDERSON, P.; KEMPE, D. R. C. 1976. Rare earth element and related chemistry of some drilled southern Indian Ocean basalts and volcanogenic sediments. *Journal of Geophysical Research* 81:4257–4268.

FODEN, J. D.; VARNE, R. 1980. The petrology and tectonic setting of Quaternary–Recent volcanic centres of Lombok and Sumbawa, Sunda Arc. *Chemical Geology* 30:201–226.

FREY, F. A.; BRYAN, W. B.; THOMPSON, G. 1974. Atlantic Ocean floor: Geochemistry and petrology of basalts from Legs 2 and 3 of the Deep Sea Drilling Project. *Journal of Geophysical Research* 79:5507–5527.

FURNES, H. 1978. Element mobility during palagonitization of a subglacial hyaloclastite in Iceland. *Chemical Geology* 22:249–264.

GELINAS, L.; BROOKS, C.; TRZCIENSKI, W. E. 1976. Archean variolites; quenched immiscible liquids. *Canadian Journal of Earth Sciences* 13:210–230.

GLEADOW, A. J. W.; DUDDY, I. E. 1980. Early Cretaceous volcanism and the early breakup history of southeastern Australia: Evidence from fission track dating of volcaniclastic sediments, *in:* CRESSWELL, M. M.; VELLA, P. (ed.). *Gondwana Five: Proceedings Fifth International Gondwana Symposium* 295–300.

GLEADOW, A. J. W.; LOVERING, J. F. 1978. Fission track geochronology of King Island, Bass Strait, Australia: Relationship to continental rifting. *Earth and Planetary Science Letters* 37:429–437.

GREEN, D. H.; LIEBERMANN, R. C. 1976. Phase equilibria and elastic properties of a pyrolite model for the oceanic upper mantle. *Tectonophysics* 32:61–92.

GREEN, D. H.; HIBBERSON, W. O.; JAQUES, A. L. 1979. Petrogenesis of mid-ocean ridge basalts, in: MCELHINNY, M. W. (ed.). *The Earth: Its origin, structure and evolution*. 265–295. Academic Press : London.

GREEN, T. H. 1980. Island arc and continent-building magmatism — a review of petrographic models based on experimental petrology and geochemistry. *Tectonophysics* 63:367–385.

GROBLER, N. J.; BOTHA, B. J. V. 1976. Pillow lavas and hyaloclastite in the Ongeluk Andesite Formation in a road cutting west of Griquatown, South Africa. *Transactions Geological Society South Africa*. 79:53–57.

HAMILYN, P. R.; KEAYS, R. R.; CAMERON, W. E.; CRAWFORD, A. J.; WALDRON, H. M. 1985. Precious metals in magnesian low-Ti lavas: Implications for metallogenesis and sulfur saturation in primary magmas. *Geochemica et Cosmochimica Acta* 49:1797–1811.

HANSON, G. N. 1977. Geochemical evolution of the suboceanic mantle. *Journal Geological Society of London* 134:235–253.

HARLEY, S. L. 1985. Garnet-orthopyroxene bearing granulites from Enderby Land, Antarctica: metamorphic pressure-temperature-time evolution of the Archaean Napier Complex. *Journal of Petrology* 26:819–856.

HAUKKA, M. T.; THOMAS, I. L. 1977. Total x-ray fluorescence analysis of geological samples using a low dilution lithium metaborate fusion method. Matrix corrections for major elements. *X-Ray Spectrometry* 6:204–211.

HELLMAN, P. L.; SMITH, R. E.; HENDERSON, P. 1979. The mobility of the rare earth elements: Evidence and implications from selected terrains affected by burial metamorphism. *Contributions to Mineralogy and Petrology* 71:23–44.

HICKEY, R.; FREY, F. A. 1979. Petrogenesis of high-Mg andesites: Geochemical evidence. *Eos* 60:413.

HONNOREZ, J.; KIRST, P. 1976. Submarine basaltic volcanism; morphometric parameters for discriminating hyaloclastites from hyalotuffs. *Bulletin of Volcanology* 39:441–465.

HUPPERT, H. E.; SPARKS, R. S. J. 1980. Restrictions on the compositions of mid-ocean ridge basalts; a fluid dynamical investigation. *Nature* 286:46–48.

ILLING, L. V.; WELLS, A. J.; TAYLOR, J. C. M. 1965. Penecontemporary dolomite in the Persian Gulf. *Special Publication Society of Economic Paleontologists and Mineralogists* 13:89–111.

JACKSON, M. C. 1980. Stratigraphy and flow morphology of Archean tholeiites, northeastern Ontario. *Precambrian Research* 12:31–41.

JACOBS, J. W.; KOROTEV, R. L.; BLANCHARD, D. P.; HASKIN, L. A. 1977. A well-tested procedure for instrumental neutron activation analysis of silicate rocks and minerals. *Journal Radioanalytical Chemistry* 40:93–114.

JAGO, J. B. 1974. The origin of Cottons Breccia, King Island, Tasmania, *Transactions Royal Society of South Australia* 98:13–28.

JAHN, B.; SUN, S. S. 1979. Trace element distribution and isotopic composition of Archean greenstones. *Physics and Chemistry of the Earth* 11:597–618.

JANECKY, D. R. 1979. Experimental seawater-peridotite interaction at 300°C, 500 bars: Implications for metallogenesis at oceanic fracture zones. *Abstracts and Programs Geological Society of America* 11:450.

JAQUES, A. L.; GREEN, D. H. 1980. Anhydrous melting of peridotite at 0–15 Kb pressure and the genesis of tholeiitic basalts. *Contributions to Mineralogy and Petrology* 73:287–310.

JENNER, G. A. 1981. Geochemistry of high-Mg andesites from Cape Vogel, Papua New Guinea. *Chemical Geology* 33:307–332.

JENNINGS, D. J.; COX, S. F. 1978. *Geological Atlas 1:250 000 series. Sheets SK55-1 and SK55-2. King Island — Flinders Island.* Department of Mines, Tasmania.

JENNINGS, D. J.; SUTHERLAND, F. L. 1969. Geology of the Cape Portland area with special reference to the Mesozoic (?) rocks. *Technical Report Department of Mines Tasmania* 13:45–82.

JORDAN, H. 1981. Metasediments and volcanics in the Frolov Ridge, Bowers Mountains, Antarctica. *Geologisches Jahrbuch Reihe B* 41:139–154.

KAY, R. W.; SENECHAL, R. G. 1976. The rare earth geochemistry of the Troodos Ophiolite Complex. *Journal of Geophysical Research* 81:964–970.

KEAYS, R. R. 1982. Archaean gold deposits and their source rocks: The upper mantle connection, *in:* FOSTER, R. P. (Ed.). GOLD '82: The geology, geochemistry and genesis of gold deposits. *Special Publication Geological Society Zimbabwe* 1:17–51.

KNIGHT, C. L.; NYE, P. B. 1953. The King Island Scheelite mine, *in:* EDWARDS, A. B. (ed.). Geology of Australian ore deposits. *Publications Fifth Empire Mining and Metallurgy Congress* 1:1222–1232.

KURODA, N; SHIRAKI, K. 1975. Boninite and related rocks of Chichi-jima, Bonin Islands, Japan. *Report Faculty Science Shizucka University* 10:145–155.

KWAK, T. A. P. 1978. Mass balance relationships and skarn-forming processes at the King Island scheelite deposit, King Island, Tasmania, Australia. *American Journal of Science* 278:943–968.

LANGMUIR, C. H.; BENDER, J. F.; BENCE, A. E.; HANSON, G. N.; TAYLOR, S. R. 1977. Petrogenesis of basalts from the FAMOUS area: mid-Atlantic Ridge. *Earth and Planetary Science Letters* 36:133–156.

LARGE, R. R. 1971. Metasomatism and scheelite mineralization at Bold Head, King Island. *Proceedings Australasian Institute of Mining and Metallurgy* 238:31–45.

LOESCHKE, J.; SCHOCK, H. H. 1980. Rare earth element contents of Norwegian greenstones and their geotectonic implications. *Norsk Geologisk Tidsskrift* 60:29–37.

LOFGREN, G. 1971. Spherulitic textures in glassy and crystalline rocks. *Journal of Geophysical Research* 76:5635–5648.

LOFGREN, G. 1974. An experimental study of plagioclase crystal morphology: Isothermal crystallization. *American Journal of Science* 274:243–273.

LONSDALE, P.; BATIZA, R. 1980. Hyaloclastite and lava flows on young seamounts examined with a submersible. *Bulletin Geological Society of America* 91:545–554.

LUDDEN, J. N.; THOMPSON, G. 1978. Behaviour of rare earth elements during submarine weathering of tholeiitic basalt. *Nature* 274:147–149.

LUDDEN, J. N.; THOMPSON, G. 1979. An evaluation of the behaviour of the rare earth elements during the weathering of sea-floor basalt. *Earth and Planetary Science Letters* 43:85–92.

MATTEY, D. P.; GIBSON, I. L.; MARRINER, G. F.; THOMPSON, R. N. 1977. The diagnostic geochemistry, relative abundance and spatial distribution of high-calcium, low-alkali olivine tholeiite dykes in the lower Tertiary regional swarm of the Isle of Skye, N.W. Scotland. *Mineralogical Magazine* 41:273–285.

MCCLENAGHAN, M. P.; SEYMOUR, D. B.; VILLA, I. M. 1994. Lamprophyre dyke suites from western Tasmania, their radiometric dating and the age of thrust faulting in the Point Hibbs area. *Australian Journal of Earth Sciences* 41:47–54.

MCDOUGALL, I.; LEGGO, P. J. 1965. Isotopic age determinations on granitic rocks from Tasmania. *Journal Geological Society Australia* 12:295–332.

MENZIES, M.; SEYFRIED, W.; BLANCHARD, D. 1979. Experimental evidence of rare earth element immobility in greenstones. *Nature* 282:398–399.

MIYASHIRO, A. 1974. Volcanic rock series in island arcs and active continental margins. *American Journal of Science* 274:321–355.

MOORE, J. G. 1975. Mechanism of formation of pillow lava. *American Scientist* 63:269–276.

NESBITT, R. W.; SUN, S. S. 1980. Geochemical features of some Archaean and post Archaean–low-alkali liquids. *Philosophical Transactions Royal Society of London* Series A, 297:365–381.

NISBET, E. G.; PEARCE, J. A. 1977. Clinopyroxene composition in mafic lavas from different tectonic settings. *Contributions to Mineralogy and Petrology* 63:149–160.

NISBET, E. G.; BICKLE, M. J.; MARTIN, A. 1977. The mafic and ultramafic lavas of the Belingwe Greenstone Belt, Rhodesia. *Journal of Petrology* 18:521–566.

NORRISH, K.; CHAPPELL, B. W. 1967. X-ray fluorescence spectrography, *in:* ZUSSMAN, J. (ed.). *Physical methods in determinative mineralogy*. 161–214. Academic Press : London.

NORRISH, K.; HUTTON, J. T. 1969. An accurate x-ray spectrographic method for the analysis of a wide range of geological samples. *Geochimica et Cosmochimica Acta* 33:431–453.

O'HARA, M. J. 1977. Geochemical evolution during fractional crystallisation of a periodically refilled magma chamber. *Nature* 266:503–507.

O'HARA, M. J.; MATHEWS, R. E. 1981. Geochemical evolution in an advancing, periodically replenished, periodically tapped, continuously fractionated magma chamber. *Journal Geological Society of London* 138:237–277.

O'NIONS, R. K.; CLARKE, D. B. 1972. Comparative trace element geochemistry of Tertiary basalts from Baffin Bay. *Earth and Planetary Science Letters* 15:436–446.

O'NIONS, R. K.; PANKHURST, R. J. 1976. Sr-isotope and Rare Earth Element geochemistry of DSDP Leg 37 basalts. *Earth and Planetary Science Letters* 31:255–261.

O'NIONS, R. K.; HAMILTON, P. J.; EVENSEN, N. M. 1977. Variations in $^{143}Nd/^{144}Nd$ and $^{87}Sr/^{86}Sr$ ratios in oceanic basalts. *Earth and Planetary Science Letters* 34:13–22.

PARSONS, W. H. 1969. Criteria for the recognition of volcanic breccias (Review). *Memoirs Geological Society of America* 115:263–304.

PEARCE, J. A. 1975. Basalt geochemistry used to investigate past tectonic environments on Cyprus. *Tectonophysics* 25:41–67.

PEARCE, J. A.; NORRY, M. J. 1979. Petrogenetic implications of Ti, Zr, Y and Nb variations in volcanic rocks. *Contributions to Mineralogy and Petrology* 69:33–47.

PERFIT, M. R.; GUST, D. A.; BENCE, A. E.; ARCULUS, R. J.; TAYLOR, S. R. 1980. Chemical characteristics of island-arc basalts: Implications for mantle sources. *Chemical Geology* 30:227–256.

POHL, D. C.; DICKSON, F. W. 1979. Experimental investigation of natural basaltic glass-seawater reactions at 400°C and 500°C and 100 bars pressure. *Abstracts and Programs Geological Society of America* 11:497.

RANKAMA, K. 1973. The late Precambrian glaciation, with particular reference to the Southern Hemisphere. *Journal and Proceedings Royal Society of New South Wales* 106:89–97.

RITTMAN, A. 1962. *Volcanoes and their activity*. John Wiley and Sons : New York.

SAUNDERS, A. D.; TARNEY, J.; MARSH, N. G.; WOOD, D. A. 1980. Ophiolites as ocean crust or marginal basin crust: A geochemical approach, in: PANAYIOTOU, A. (ed.). *Ophiolites. Proceedings International Ophiolite Symposium, Cyprus, 1979*. 193–204. Ministry of Agriculture and Natural Resources : Cyprus. 193–204.

SCHERMERHORN, L. J. G. 1966. Terminology of mixed coarse-fine sediments. *Journal Sedimentary Petrology* 36:831–835.

SCHILLING, J-G. 1975. Azores mantle blob: rare-earth evidence. *Earth and Planetary Science Letters* 25:103–115.

SCHILLING, J-G.; NOE-NYGAARD, A. 1974. Faeroe-Iceland plume: Rare-earth evidence. *Earth and Planetary Science Letters* 24:1–14.

SCHMINCKE, H. U.; ROBINSON, P. T.; OHNMACHT, W.; FLOWER, M. F. J. 1979. Basaltic hyaloclastites from hole 396B, DSDP Leg 46. *Initial Report Deep Sea Drilling Project* 46:341–356.

SCHWARZ, E. J.; FUJIWARA, Y. 1977. Komatiitic basalts from the Proterozoic Cape Smith Range in northern Quebec, Canada. *Special Papers Geological Association of Canada* 16:193–201.

SCOTT, B. 1951. The petrology of the volcanic rocks of south east King Island, Tasmania. *Papers and Proceedings Royal Society of Tasmania* 85:113–136.

SHIRAKI, K.; KURODA, N. 1977. The boninite revisited. *Journal Geography (Tokyo)* 86(3):34–50.

SMEWING, J. D.; POTTS, P. J. 1976. Rare-earth abundances in basalts and metabasalts from the Troodos Massif, Cyprus. *Contributions to Mineralogy Petrology* 57:245–258.

SMEWING, J. D.; SIMONIAN, K. O.; GASS, I. G. 1975. Metabasalts from the Troodos Massif, Cyprus: Genetic implications deduced from petrography and trace element geochemistry. *Contributions to Mineralogy and Petrology* 51:49–64.

SOLOMON, M. 1969. The nature and possible origin of the pillow lavas and hyaloclastite breccias of King Island, Australia. *Journal Geological Society of London* 124:153–169.

SPARKS, R. S. J.; MEYER, P.; SIGURDSSON, H. 1980. Density variation amongst mid-ocean ridge basalts: Implications for magma mixing and the scarcity of primitive lavas. *Earth and Planetary Science Letters* 46:419–430.

STRONG, D. F.; DOSTAL, J. 1980. Dynamic melting of Proterozoic upper mantle: Evidence from rare earth elements in oceanic crust of eastern Newfoundland. *Contributions to Mineralogy and Petrology* 72:165–173.

SUN, S. S. 1980. Lead isotopic study of young volcanic rocks from mid-ocean ridges, ocean islands and island arcs. *Philosophical Transactions Royal Society of London* Series A, 297:409–445.

SUN, S-S.; HANSON, G. N. 1975. Origin of Ross Island basanitoids and limitations upon the heterogeneity of mantle sources for alkali basalts and nephelinites. *Contributions to Mineralogy and Petrology* 52:77–106.

SUN, S-S.; NESBITT, R. W. 1978. Petrogenesis of Archaean ultramafics and basic volcanics: Evidence from rare earth elements. *Contributions to Mineralogy and Petrology* 65:301–325.

SUN, S-S.; NESBITT, R. W.; SHARASKIN, A. Ya. 1979. Geochemical characteristics of mid-ocean ridge basalts. *Earth and Planetary Science Letters* 44:119–138.

SUTHERLAND, F. L.; CORBETT, E. B. 1974. The extent of Upper Mesozoic igneous activity in relation to lamprophyric intrusions in Tasmania. *Papers Proceedings Royal Society Tasmania* 107:175–190.

THOMAS, I. L.; HAUKKA, M. T. 1978. XRF determination of trace and major elements using a single-fused disc. *Chemical Geology* 21:39–50.

THOMSON, B. P. 1969. Precambrian basement cover: The Adelaide System, *in:* PARKIN, L. W. (ed.). *Handbook of South Australian Geology* 49–84. Geological Survey of South Australia.

VARNE, R.; FODEN, J. D. 1987. Tectonic setting of Cambrian rifting, volcanism and ophiolite formation in western Tasmania. *Tectonophysics* 140:275–295.

WALDRON, H. M. 1977. *The geology of part of south east King Island and thermodynamic modelling and metallogenesis of mid-ocean ridge system*s. B.Sc. (Hons) Thesis, University of Melbourne.

WALDRON, H. M.; BROWN, A. V. 1986. Major, trace and REE chemistry of Eocambrian–Cambrian basaltic suites from the Dundas Trough and Smithton Basin, western Tasmania. *Unpublished Report Department of Mines Tasmania* 1986/86.

WALKER, D.; POWELL, M. A.; LOFGREN, G. E.; HAYS, J. F. 1978. Dynamic crystallization of a eucrite basalt. *Proceedings of the 9th Lunar and Planetary Science Conference* 1369–1391.

WATERHOUSE, L. L. 1916. Notes on geology of King Island. *Report Secretary for Mines Tasmania* 1915:88–93.

WILKINSON, J. F. G. 1982. The genesis of mid-ocean ridge basalts. *Earth Science Reviews* 18:1–57.

WILLIAMS, E. 1978. Tasman Fold Belt system in Tasmania. *Tectonophysics* 48:159–205.

WILLIAMS, G. E. 1979. Sedimentology, stable-isotope geochemistry and palaeoenvironment of dolostones capping late Precambrian glacial sequences in Australia. *Journal Geological Society Australia* 26:377–386.

WOOD, D. A. 1978. Major and trace element variations in the Tertiary lavas of eastern Iceland and their significance with respect to the Iceland geochemical anomaly. *Journal of Petrology* 19:393–436.

WOOD, D. A. 1979. Dynamic partial melting; its application to the petrogenesis of basalts erupted in Iceland, the Faeroe Islands, the Isle of Skye (Scotland) and the Troodos Massif (Cyprus). *Geochimica et Cosmochimica Acta* 43:1031–1046.

WOOD, D. A. 1981. Partial melting models for the petrogenesis of Reykjanes Peninsula Basalts, Iceland: Implications for the use of trace elements and strontium and neodymium isotope ratios to record inhomogeneities in the upper mantle. *Earth and Planetary Science Letters* 52:183–190.

WOOD, D. A.; GIBSON, I. L.; THOMPSON, R. N. 1976. Elemental mobility during zeolite facies metamorphism of the Tertiary basalts of eastern Iceland. *Contributions to Mineralogy and Petrology* 55:241–254.

[15 September 1993]